

# Life cycle assessment of a process for paracetamol flow synthesis from bio-waste derived $\beta$ -pinene

Sabine Hallamasek,<sup>1</sup> Vera Ubbenjans<sup>1,2</sup> and Alexei A. Lapkin<sup>1,3,\*</sup>

<sup>1</sup>*Department of Chemical Engineering and Biotechnology, University of Cambridge, Philippa Fawcett Drive, Cambridge CB3 0AS, UK*

<sup>2</sup>*Aachener Verfahrenstechnik - Process Systems Engineering (AVT.SVT), RWTH Aachen University, 52074 Aachen, Germany*

<sup>3</sup>*Cambridge Centre for Advanced Research and Education in Singapore, CARES Ltd. 1 CREATE Way, CREATE Tower #05-05, 138602 Singapore*

## Abstract

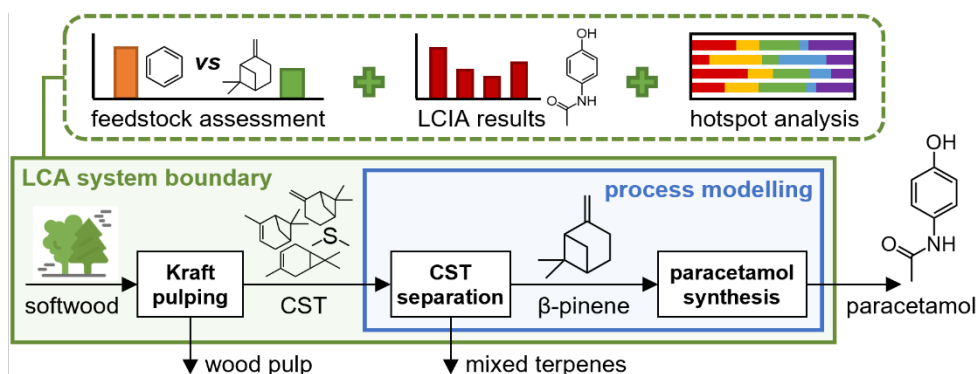
The synthesis of functional molecules from bio-waste feedstocks with retention of key structural molecular motifs is a potentially effective strategy to replace conventional fossil-based synthesis routes. In this work we are focusing on the synthesis of functional molecules from terpenes, a class of underutilised bio-waste molecules generated, for instance, as a by-product of Kraft paper pulping. Recent literature studies demonstrated a possible pathway for a continuous flow synthesis of paracetamol from  $\beta$ -pinene. While this process is currently not of commercial interest, the available literature synthesis demonstrates the technical feasibility of such chemical conversion as well as several new chemical transformations. However, the environmental efficiency of the proposed flow synthesis was not determined. Here, we perform a life cycle assessment to quantify the environmental impacts of a potential industrial-scale paracetamol manufacture from bio-waste  $\beta$ -pinene. For this purpose, scaled-up process models of continuous paracetamol manufacture were developed in Aspen Plus and a complete life cycle inventory was estimated. A GWP of 58 kg CO<sub>2</sub>-eq./kg product was predicted, and key impact contributing aspects of the designed process were identified through a hotspot analysis. A comparative feedstock analysis showed that  $\beta$ -pinene derived from Kraft pulping waste can be a cleaner feedstock than the benchmark feedstock benzene. The obtained LCA results represent highly conservative estimates, given the early design stage, and thus promise to surpass standard industry practises, once optimised. The results

---

\* Corresponding author; Email: aal35@cam.ac.uk

presented in this study can serve as a basis for comparison against conventional paracetamol production LCA datasets.

## Graphical Abstract



**Keywords:** life cycle assessment; process modelling; green chemistry; biomass feedstock; flow chemistry; life cycle inventory

## 1. Introduction

Progressive anthropogenic degradation of the environment combined with continuous population growth and limited availability of material resources urges a transition towards a chemical industry based on bio-renewable feedstocks.<sup>1–3</sup> Today, the majority of chemicals and polymers are manufactured from fossil feedstocks, not least because the cost of bio-based production often exceeds the cost of petrochemical processes.<sup>4,5</sup> However, increasingly volatile prices of fossil resources and a competitive petrochemical market provide an economic incentive for the transition to bio-renewable feedstocks, in addition to the environmental and social benefits gained from this shift.<sup>6–8</sup> Several policy documents have been published that reflect the desire to reduce industrial dependencies on fossil feedstocks, such as the EU Green Deal,<sup>9</sup> the Industrial Strategy for Europe<sup>10,11</sup> and the UN Sustainable Development Goals.<sup>12</sup>

One interesting source of naturally abundant, bio-renewable organic molecules is turpentine, a mixture of volatile organic substances obtained from wood biomass. The main components of turpentine are monoterpenes, a class of energy-dense unsaturated hydrocarbons made up of two isoprene units<sup>4,13</sup> that has the potential to serve as alternative feedstock material for

chemical processes. While the exploitation of monoterpenes for lower value applications has been widely investigated in the literature, the conversion of terpenes into structurally similar functional molecules based on green chemistry principles is a rather recent subject.

Here, an interesting case study is the continuous flow synthesis of the functional molecule paracetamol from the monoterpene  $\beta$ -pinene. The bench-scale technology of this process was conceptualised at the University of Bath and is described in more detail in the supporting materials. This synthesis pathway represents a proof-of-concept that could pave the way for terpene-based manufacture of a range of functional molecules. However, the environmental impacts associated with this synthesis were not previously quantified, which is an essential task to determine whether an industrial process based on this synthesis route could yield a green alternative to conventional paracetamol manufacture. As such, the core research goal of this study was to holistically evaluate the environmental impacts of this proof-of-concept process for the manufacture of paracetamol from  $\beta$ -pinene at the industrial scale.

#### *Turpentine – availability, processing, applications*

The global annual production of turpentine for the last 15 years lies at 300 000 – 350 000 t/year, some of which is obtained from the tapping of live trees (“gum turpentine”) and from the distillation of wood stumps. The majority of turpentine (60 – 70%), however, is generated as a by-product from the Kraft pulping process,<sup>4,14,15</sup> the globally prevailing paper manufacturing process. With a production of more than 100 million tons of Kraft pulp per annum, the Kraft pulping process accounts for more than 60% of the worldwide pulp production.<sup>4,16</sup> During Kraft pulping, softwood is cooked in an alkaline sodium sulphide solution inside a pressurized digester to extract cellulose fibres for paper production. Hereby, “crude sulphate turpentine” (CST) is obtained by capturing the relief vapours of the digester, which are composed of biomass monoterpenes and sulphur compounds that stem from the cooking solution. On average, 3 – 15 kg CST can be obtained per tonne of Kraft pulp, depending on the origin and type of wood used.<sup>4,13,16</sup> For Scandinavia, where most of the European Kraft pulping takes place, the average CST yield from Kraft pulping is about 10 kg/t pulp.<sup>13</sup> The obtained bio-waste CST is commonly sold to industry for low value applications, with about 30% of commercially sold CST produced in Europe.<sup>4</sup> In 2017, the market price of CST was approximately £170/t,<sup>17</sup> which is significantly lower than the price of fossil resources in the

same year, when a barrel of crude oil cost on average \$54 (Europe Brent, ~\$400/t)<sup>6</sup> and the commonly employed fossil-derived feedstock benzene cost \$830/t.<sup>18–20</sup> Notably, the prices of both these commodities have since increased to \$108/barrel<sup>6</sup> and \$1500/t<sup>18,21,22</sup> on average, respectively (Jan-Jul 2022). As such, CST is not only a bio-renewable and locally available, but also a cheap source of organic molecules.

Before CST can be processed into value-added products it must be desulphurised, as its sulphurous compounds may otherwise cause numerous downstream issues including catalyst poisoning, malodour, and sulphur dioxide formation upon combustion. Generally, desulphurisation to less than 5 ppm sulphur content is desirable, and common desulphurisation methods include distillation (industrially prevalent), oxidation, and extraction.<sup>23–25</sup> The isolated sulphur compounds, including oxidation products such as sulfonyl chlorides, thiosulfonates and dimethyl sulfoxide, may be sold to other industries for various applications.<sup>26</sup> At many pulp mills, desulphurised turpentine is simply burnt for energy recovery as an effective way of treating turpentine bio-waste while reducing fuel costs of running the Kraft process.<sup>4</sup>

However, turpentine is also a frequently employed renewable feedstock material. Without further separation, turpentine is mainly used to solvate and reclaim rubber, as solvent in paints and varnishes or in other chemical solvent applications.<sup>13,16,27</sup> Unseparated turpentine can also be used as a fuel additive to improve engine performance,<sup>4</sup> or to produce motor and aviation bio-fuels *via* terpene hydrogenation.<sup>15,28</sup>

Separation of turpentine into its individual monoterpene fractions yields significant portions of purified  $\alpha$ -pinene and  $\beta$ -pinene. This separation is generally done through ordinary or vacuum distillation which, due to proximity in terpene boiling points, is rather energy intensive.<sup>4,13,27</sup> While  $\beta$ -pinene shows higher reactivity than the more abundant  $\alpha$ -isomer due to the presence of the exocyclic double bond, both pinenes can be interconverted through catalytic isomerisation.<sup>14,29</sup> The obtained monoterpene fractions are commonly used starting materials for chemical synthesis, including the production of fragrances,<sup>29</sup> flavorings<sup>30</sup> and polyterpene resins.<sup>14</sup>  $\alpha$ -Pinene is mainly used for the synthesis of pine oil ( $\alpha$ -terpineol), but is also employed to prepare menthol, isoborneol and camphor.<sup>13,27</sup>  $\beta$ -Pinene is a common

precursor for commercially produced fragrances as it can be pyrolyzed to  $\beta$ -myrcene from which geraniol, nerol, or linalool can be derived.<sup>13,27</sup> Medicinal applications of turpentine and its derivatives include the production of liniments from turpentine oil<sup>16</sup> and the use of  $\alpha$ -terpineol as anti-septic,<sup>27</sup> however, the potential that terpenoids hold as feedstocks for the synthesis of small molecule pharmaceuticals is still rather unexplored.

Recent literature on potentially viable alternative applications of CST demonstrate its use as feedstock for the synthesis of functionalised molecules. Several protocols for the direct conversion of untreated CST into valuable synthetic building blocks have been developed, which circumvents the costly separation of CST into terpene fractions via distillation. This includes the conversion of CST-contained monoterpenes into p-menthadienes,<sup>31</sup> which are valuable intermediates for the synthesis of p-cymene<sup>32</sup> and terephthalic acid,<sup>33</sup> as well as the direct epoxidation of monoterpenes in CST to yield terpene epoxides,<sup>34,35</sup> which may be transformed into a range of functionalised compounds via selective reaction protocols.<sup>36</sup>

#### *Synthesis of paracetamol as a globally used API*

In this study, we investigated the environmental impacts of a case study process for the synthesis of paracetamol from CST-derived  $\beta$ -pinene. With a production volume exceeding 100 000 t/y, paracetamol is one of the most commonly sold over-the-counter drugs and represents a key active ingredient within the pharmaceutical industry.<sup>37,38</sup> Industrially, paracetamol is widely synthesised *via* N-acetylation of 4-aminophenol,<sup>39</sup> which can be obtained from the benzene derivatives nitrobenzene, 4-nitrophenol and 4-nitrochlorobenzene through various chemical routes.<sup>40–42</sup> Another established paracetamol synthesis method is the Hoechst-Celanese process,<sup>43</sup> where the substrate 4-hydroxyacetophenone is also generally manufactured from benzene derivatives such as phenol.<sup>44</sup> Since benzene is conventionally gained from crude oil,<sup>45</sup> current paracetamol manufacture is essentially based on fossil feedstocks. This dependency on fossil-derived feedstock compounds in the synthesis of functionalised molecules is an industry-wide issue that incurs hard-to-abate carbon emissions across the upstream manufacturing process. The resulting presence of embedded carbon in the final product molecule contributes to Scope 3 emissions which typically constitute the largest proportion of emissions across a product's life cycle evaluation.<sup>46</sup> As such, a new pathway for paracetamol synthesis from bio-waste  $\beta$ -pinene

feedstock that has reduced environmental impacts would support a transition away from petrochemical dependence and promote the bio-based manufacture of functionalised molecules.

Investigating the synthesis of paracetamol from CST-derived  $\beta$ -pinene is also relevant to recent policy objectives on reshoring pharmaceutical manufacture back to local production sites, such as described in the European pharmaceutical strategy of 2020.<sup>47</sup> Current paracetamol production sites are predominantly located in India and China and have a production output of 2 000 – 40 000 t/y,<sup>48–52</sup> while there is no active production of commercial paracetamol API in Europe.<sup>48,53,54</sup> However, there is a growing interest to decentralise pharmaceutical production to generate shorter value chains and support regional pharmaceutical autonomy. This notion is mainly driven by social and environmental benefits that can be attained from this proposition, such as secured access to high-quality medicines and reductions in transportation related emissions.<sup>47</sup> As CST is a biomass-based feedstock widely available in Europe and other regions, the synthesis of paracetamol from CST-derived  $\beta$ -pinene offers a potentially feasible close-to-market manufacturing option. Additionally, this case study could inspire the local manufacture of other pharmaceuticals through terpene-based methods.

### *Aims of this study*

To obtain the benefits of functional molecule synthesis from locally sourced bio-renewables, efficient and clean process operation is imperative. In this work we calculated the environmental impacts of an industrial-scale flow synthesis process for the manufacture of paracetamol from CST-derived  $\beta$ -pinene. For this purpose we used the Life Cycle Assessment (LCA) methodology, a widespread and standardized tool to evaluate environmental process impacts across various life cycle stages.<sup>55,56</sup> To quantify the required Life Cycle Inventory (LCI), it was necessary to develop models of every step of the proposed process using experimental and literature data, from which values of material consumption, energy requirements and process emissions could be extracted. The obtained LCI data was employed to conduct cradle-to-gate LCA of the proposed process, the results of which were used to: (i) compare the environmental efficiency of the CST-derived  $\beta$ -pinene feedstock to petrochemical-based benzene feedstock, (ii) estimate the environmental burdens of the  $\beta$ -pinene-based

paracetamol manufacturing process, and (iii) identify hotspots of the case study process to guide future process optimisation.

## 2. Experimental

### 2.1 Synthesis of paracetamol from $\beta$ -pinene at the bench-scale

The synthesis of paracetamol from  $\beta$ -pinene proceeds *via* six distinct processing steps. Each step consists of a reaction followed by a separation procedure to isolate the target products.

The overall route is shown in Scheme 1, and proceeds as follows:

- Step I:  $\beta$ -pinene is diluted in a methanol-water mixed solvent and is converted to nopinone *via* ozonolysis at 20 °C and 1 bar.
- Step II: Nopinone is reacted with trimethyl orthoformate (TMOF) at 45 °C and 1 bar in the presence of 98 wt.% H<sub>2</sub>SO<sub>4</sub>, inducing an acid-catalysed ring-opening reaction. This yields isomeric intermediates 4-isopropenylcyclohexanone (IPC) and 4-isopropylidenecyclohexanone (IPCD).
- Step III: The product mixture of IPC and IPCD is converted into a mixture of 4-acetylcyclohexanone (ACH) and 1,4-cyclohexanedione (CHD), respectively, *via* ozonolysis at 20 °C and 1 bar in a methanol-water mixed solvent.
- Step IV: The mixture of ACH and CHD is diluted in diethylene glycol dibutyl ether (DEGDBE) and dehydrogenated to form the aromatic compounds 4-hydroxyacetophenone (HAP) and hydroquinone (HQ), respectively, using a Pd/C catalyst packed bed at 230 °C and 4 bar with a continuous N<sub>2</sub> flush for H<sub>2</sub> venting.
- Step V: HAP is converted to paracetamol *via* a solvent-free one-pot oximation and Beckmann-rearrangement with hydroxylamine hydrochloride (HAHCL) at 110 °C and 1 bar.
- Step VI: HQ is converted to paracetamol *via* amidation with ammonium acetate in acetic acid at 220 °C and 10 bar.

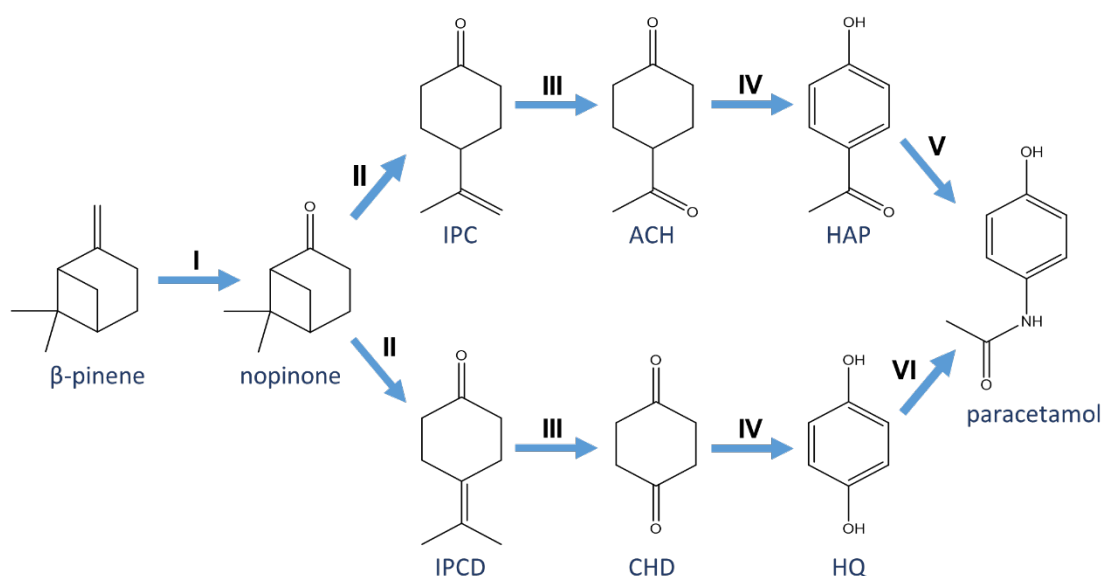
Details of the bench-scale reaction conditions, experimental results and sources of experimental data are given in Table S1 of the Supporting Information (SI). The separation strategies employed during the bench-scale experiments to isolate intermediate products for further processing are given in

Table 1. An overview of the reaction and separation strategies employed during synthesis steps I – VI. Separation strategies marked with an asterisk were proposed but not experimentally tested during bench-scale investigations.

| <b>Synthesis Step</b> | <b>Reactions</b>                            | <b>Bench-scale separation strategies</b>                               |
|-----------------------|---|--|
| Step I                | Liquid-phase ozonolysis                     | Membrane separation, rotary evaporation                                |
| Step II               | Acid-catalysed ring-opening                 | Decantation  |
| Step III              | Liquid-phase ozonolysis                     | Membrane separation, rotary evaporation                                |
| Step IV               | Pd/C catalysed liquid-phase dehydrogenation | Reactive extraction, decantation, fractional crystallisation in water* |
| Step V                | One-pot oximation-Beckmann rearrangement    | Crystallisation in water*  |
| Step VI               | Amidation                                   | Distillation, crystallisation  |

Experimental analysis of reaction yields showed that significant amounts of side product species are generated during each reaction step. Unfortunately, not all side products were quantified in the data sources used for this study. Additionally, while the synthesis concept of paracetamol from  $\beta$ -pinene was designed to work in continuous flow operation, experimental investigation of each step was carried out individually, rather than as a combined flow process. As such, the behaviour of by-products throughout downstream processing steps was not experimentally investigated. An overview of the experimental observations with regards to the impurities formed across this synthesis route is given in Table S1.





Scheme 1. Reaction pathway for the synthesis of paracetamol from  $\beta$ -pinene.

Table 1. An overview of the reaction and separation strategies employed during synthesis steps I – VI. Separation strategies marked with an asterisk were proposed but not experimentally tested during bench-scale investigations.

| Synthesis Step | Reactions                                   | Bench-scale separation strategies                                      |
|----------------|---|--|
| Step I         | Liquid-phase ozonolysis                     | Membrane separation, rotary evaporation                                |
| Step II        | Acid-catalysed ring-opening                 | Decantation  |
| Step III       | Liquid-phase ozonolysis                     | Membrane separation, rotary evaporation                                |
| Step IV        | Pd/C catalysed liquid-phase dehydrogenation | Reactive extraction, decantation, fractional crystallisation in water* |
| Step V         | One-pot oximation-Beckmann rearrangement    | Crystallisation in water*  |
| Step VI        | Amidation                                   | Distillation, crystallisation  |

## 2.2 Aspen Plus process modelling; property estimation set-up

In order to obtain the cradle-to-gate process flow data for the industrial manufacture of paracetamol from CST-derived  $\beta$ -pinene, an up-scaled model of the novel process was

constructed in Aspen Plus V10 using the available bench-scale experimental and literature data. To attain reliable process modelling results, appropriate selection of thermodynamic and physicochemical property estimation methods is essential. In the interest of transparency and reproducibility of the constructed process model, choices and reasoning for selected property estimation methods are outlined below.

### *Thermodynamic modelling*

Examination of the Aspen Plus V10 databases showed that VLE data for the process species was scarce. To select appropriate thermodynamic modelling methods the stream compositions and operating conditions of all process steps were considered. As all unit operations involve significant amounts of polar compounds and some include electrolytic species, non-ideal mixing was expected within all liquid process streams.

For non-electrolytic, low-pressure unit operations (< 10 bar) activity coefficient models were selected to model phase equilibria. At low pressure and low data availability, these models commonly predict phase equilibria involving non-ideal liquids more accurately than equations of state (EOS).<sup>57</sup> Suitability of using activity coefficient models for the relevant operating temperatures was confirmed by calculating the reduced temperature  $T_r$  using Kay's rule (eq. 1), which did not exceed 0.75 for all modelled process steps. At  $T_r > 0.75$  liquids expand rapidly, and the accuracy of activity coefficient models – designed to model characteristic liquid phase interactions – would reduce.<sup>58</sup> The NRTL activity coefficient model was chosen for simulations as it is capable of modelling VLE and LLE, and has been found to outperform UNIQUAC and Wilson for VLE modelling of most mixtures relevant to this study, especially aqueous organics.<sup>59</sup> To estimate the NRTL binary interaction parameters  $\alpha$  and  $\tau$  of component pairs for which the Aspen Plus V10 databases did not hold regressed model coefficients,  $\alpha$  was set to the recommended documentation value (0.2 for LLE systems; 0.3 for non-associative, slightly non-ideal liquid mixtures of non-polar and polar compounds),<sup>60</sup> and  $\tau$  was regressed by Aspen Plus's property constant estimation system (PCES) using binary infinite-dilution activity coefficients estimated from the UNIFAC or UNIFAC-LL group contribution method.<sup>60,61</sup> For component pairs where PCES-derived parameters yielded unreasonable LLE simulations,  $\alpha$  and  $\tau$  were instead estimated from proxy data, as shown in SI Section S2.2.

$$T_r = \frac{T}{\sum y_i T_{crit,i}} \quad (1)$$

For process steps involving electrolytes the ElecNRTL extension to the NRTL model provided by Aspen Plus was employed, which accounts for ion-dipole interactions, long-range electrostatic interactions, and electrolyte reaction equilibria alongside conventional molecular interactions. ElecNRTL is applicable for aqueous and mixed-solvent systems at low pressures (< 10 bar) across wide ranges of electrolyte concentration and temperature,<sup>60</sup> has received wide industrial acceptance and has been shown to model VLE reasonably well for various systems.<sup>62</sup> To calculate phase equilibria, the ElecNRTL model requires NRTL parameters  $\alpha$  and  $\tau$  for all compound pairs. For molecule-electrolyte pairs with unknown parameter values, the  $\tau$  values ( $\tau_{mol,elec}$ ,  $\tau_{elec,mol}$ ) were set to (8, -4) for water-ion pairs, (10, -2) for solvent-ion pairs with good ionic solvation, and (5, 5) for solvent-ion pairs with poor solubility, as suggested in Aspen's documentation.<sup>60</sup> For  $\alpha$ , the model's default value (0.2) was accepted. The electrolyte equilibria considered for each process step are given in the process model descriptions in SI Section S3.

To calculate VLE within the only high-pressure unit operation ( $P \geq 10$  bar) included in this study, the step VI amidation reactor, the SR-POLAR EOS was employed. A summary of the thermodynamic modelling methods employed for the simulation of each process step is given in Table S2.

Across all simulations, Henry's law was applied to model the dissolution of light gases in liquid solvents at low concentrations. In this study, O<sub>2</sub>, N<sub>2</sub>, CO<sub>2</sub>, H<sub>2</sub>, HCl were defined as Henry components when their  $T_{crit}$  lay near or above operating temperature. The value of the temperature-dependent Henry's constant for each solute-solvent pair was calculated from Aspen database parameters where available, and otherwise estimated from proxy data as outlined in SI Section S2.3.

#### *Vapour phase description*

The gas phase was treated as real rather than ideal throughout simulations to enable modelling of non-ideal vapour phase mixing, which can bring improvement in estimation accuracy at low computational cost. For unit operations where no vapour phase association

was expected the Redlich-Kwong EOS was used, which is generally accurate for systems where the reduced pressure is less than half the reduced temperature ( $P/P_c < T/2T_c$ ), as was the case for this study. For process steps with expected vapour phase association the Hayden-O'Connell EOS was employed.

#### *Other physicochemical properties*

Several process components were not available in the Aspen Plus V10 compound databases or had incomplete entries of their physicochemical properties. Non-databank compounds were added *via* definition of their molecular structures (Table S5) and missing compound properties were entered manually where known (Tables S6 and S7). To estimate unknown pure-component and mixture properties needed for process simulation, the default sets of physicochemical property estimation methods recommended by Aspen for the selected thermodynamic model (NRTL-RK, ElecNRTL-RK, ...) were accepted. Missing property model parameters were estimated by Aspen Plus PCES where possible.

### **2.3 Aspen Plus process modelling; process model development**

The proposed manufacturing route for the synthesis of paracetamol from CST-derived  $\beta$ -pinene was modelled in Aspen Plus V10 as a continuously operating industrial-scale manufacturing plant.

#### *Aspen Plus model for the thermal separation of $\beta$ -pinene from CST*

This LCA study was based on proof-of-concept-research investigating paracetamol synthesis from purified terpenes under the assumption that terpene isolation from CST is practicably attainable. As such no primary experimental data on  $\beta$ -pinene isolation from CST was recorded as part of this project. Additionally, to the best of our knowledge, established process data for  $\beta$ -pinene isolation from CST has not been published in the literature at the time of this LCA study. To estimate the impacts incurred from CST-derived  $\beta$ -pinene within the presented cradle-to-gate LCA study in the absence of experimental data, a CST fractionation train for  $\beta$ -pinene isolation was designed based on VLE predictions, inspired by a limonene thermal separation system previously described by Helmdach et al.<sup>17</sup>

The CST distillation system was modelled in Aspen Plus using the NRTL-RK property method. The CST composition considered for this study is given in Table 2. All columns were modelled using Aspen's rigorous RadFrac blocks, with initial estimates of column specifications obtained from Aspen's DSTWU shortcut block. For each column a pressure drop of 0.0069 bar (=0.1 psi) per stage was assumed, as commonly done in the literature.<sup>63</sup> Heat integration was not considered. The designed fractionation model for the thermal separation of  $\beta$ -pinene from CST consists of seven distillation columns, and a process flow diagram of the developed fractionation train is shown in Figure 1. A detailed model description is provided in SI Section S3.1.

Table 2. Average CST composition of Northern European softwood, adapted from Helmdach et al.<sup>17</sup>

| Compound          | Content [wt. %] | Boiling point [°C] |
|-------------------|-----------------|--------------------|
| $\alpha$ -pinene  | 60.0            | 156                |
| $\beta$ -pinene   | 6.0             | 166                |
| 3-carene          | 20.0            | 168-169            |
| limonene          | 2.5             | 177                |
| sulphur compounds | 5.5             | 6-110              |

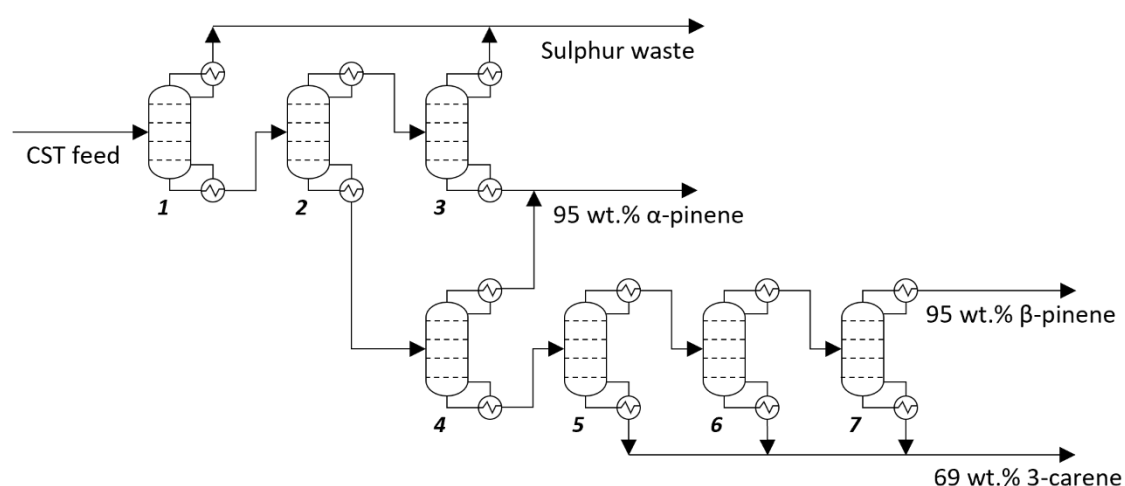


Figure 1. CST fractionation train for the isolation of  $\beta$ -pinene.

*Aspen Plus models for process steps I – VI*

The process models for steps I – VI were constructed in separate Aspen Plus simulation files to ensure quick model convergence. All simulations were based on the experimental data sets summarised in Table S1. Data gaps were supplemented with literature data. Where appropriate, experimental reactor and separation technologies were adopted in the scaled-up process models. Elsewhere, bench-scale technologies were substituted with unit operations more suitable for large throughputs. Where required, Aspen Plus simulations were supplemented with external modelling calculations in MS Excel. To simulate continuous operation of the overall process, simulations of process steps I to VI were run in sequence by manually transferring stream specifications of connecting intermediate flows. Plant-wide heat integration was not considered. The developed process flowsheet is given in Figure 2. A detailed description of the process models constructed for each process step is provided in SI Sections S3.2 – S3.7.

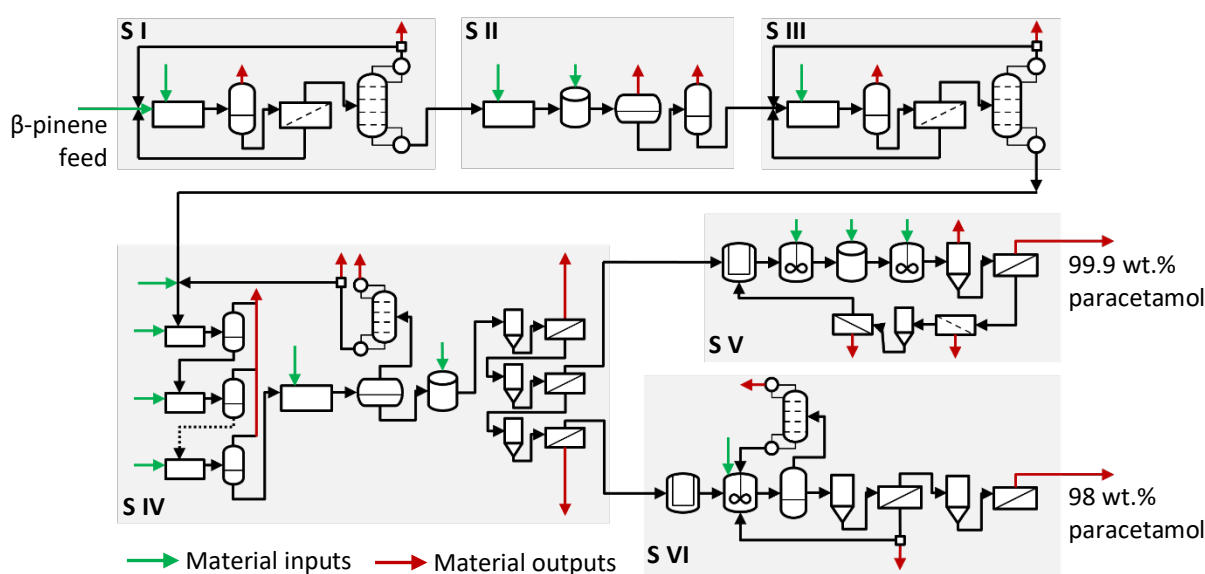


Figure 2. Process flow diagram for the continuous synthesis of paracetamol from  $\beta$ -pinene *via* process steps I – VI.

#### 2.4 Extracting life cycle inventories from the Aspen Plus process models

To obtain gate-to-gate inventories for the investigated process, the constructed Aspen models were used to calculate the material and energy flows entering and leaving the CST fractionation process, and process steps I – VI. The calculated flows were tabulated and normalised to 1 kg product output of each respective process step, generating process LCIs

for the isolation of  $\beta$ -pinene from CST (Table 3) and the manufacture of intermediates from process steps I – VI (SI Section S4.2, Tables S29 – S34). A summarised LCI for paracetamol production from  $\beta$ -pinene across steps I – VI was obtained by scaling the process inputs into steps I – VI such that the Aspen simulations yielded a total output of 1 kg paracetamol product from process steps V and VI (Table 4).

The process flows tabulated in the constructed process LCIs were rounded to three significant figures. To support data transparency, future process development and clear impact allocation, the generated LCIs explicitly list the contributions of each unit operation to the total utility consumption of a process step. Within each LCI table, generic utilities were used to characterise the heating and cooling requirements of a process. These utilities are described in Table S28 of the Supplementary Information.

## 2.5 Modelling waste treatment processes

The treatments of aqueous and organic waste streams generated throughout the paracetamol synthesis process were not investigated experimentally, thus no primary data was available to estimate the environmental impacts of treating process wastes. Furthermore, no suitable pre-assembled LCI datasets for industrial waste treatment were available in ecoinvent v3.7 to approximate the impacts of waste treatment. To obtain a cradle-to-gate LCA for the novel process without available primary or proxy data on waste treatment processes, inventory models for waste treatment were constructed using literature-derived LCI models, as outlined below.

### *Modelling the treatment of organic wastes*

Organic waste incineration was modelled to take place in a thermal waste treatment plant with energy recovery, assuming complete combustion of all organics to CO<sub>2</sub>, H<sub>2</sub>O and NO<sub>2</sub> (combustion equations are listed in Table S35). Oxygen was supplied from the gaseous exhaust streams leaving process steps I and III, which are rich in molecular oxygen (83.6 wt.%) and yield an oxygen-to-combustibles molar ratio of  $\lambda = 1.12$ , supporting complete combustion. Employing process exhausts from steps I and III as oxygen sources yields the additional benefit of effectively treating effluent ozone contained in those streams, as ozone, which is hazardous to human health, readily decomposes to oxygen at elevated temperatures.<sup>64</sup> The direct

emissions of the thermal treatment of organic wastes and ozone were calculated per kg product produced from each process step, and are given in Table S36. Non-specific process emissions and consumed auxiliaries of thermal waste treatment were estimated from the *multi-input allocation model for thermal treatment of waste solvents* presented by Seyler et al.,<sup>65</sup> which provides waste composition-dependent consumption and emission factors to calculate waste-specific LCIs for organic waste incineration. The model factors were derived from industrial case study data of a Swiss solvent waste treatment plant consisting of a combustion chamber plus a flue gas treatment facility, which was assumed representative of European organic waste incineration sites today. When using the model by Seyler et al. to estimate a process inventory for the incineration of organic waste from the flow paracetamol synthesis process, an average composition of all organic process effluents was employed as it was assumed that organic wastes would be mixed before incineration. Detailed modelling calculations for waste-specific LCI development are described in SI Section S5.

#### *Modelling the treatment of aqueous wastes*

The treatment of aqueous process wastes was modelled based on the *Input-Dependent Life-Cycle Inventory Model of Industrial Wastewater-Treatment Processes in the Chemical Sector* presented by Köhler et al.<sup>66</sup> Based on operational data from a large wastewater purification site in Germany, Köhler et al. established causal relationships between the properties of aqueous wastes and the process flows across wastewater treatment technologies. These relationships are expressed as transfer coefficients, which describe the partition of wastewater inputs into process outputs such as emissions to air and water, and consumption factors, which predict auxiliary consumption and co-product production during wastewater treatment based on wastewater-specific properties. The parameters employed by Köhler et al. to describe wastewater properties include wastewater volume, total organic carbon ( $\text{TOC}_{\text{total}}$ ,  $\text{TOC}_{\text{degradable}}$ ,  $\text{TOC}_{\text{refractory}}$ ), adsorbable organically bound halogens (AOX), nitrogen compounds ( $\text{N}_{\text{total}}$ ,  $\text{NH}_4^+\text{-N}$ ,  $\text{NO}_3^-\text{-N}$ ,  $\text{NO}_2^-\text{-N}$ ), phosphorus compounds ( $\text{PO}_4^{3-}\text{-P}$ ); heavy metals ( $\text{Cu}_{\text{total}}$ ,  $\text{Cr}_{\text{total}}$ ), and inorganic anions ( $\text{Cl}^-$ ,  $\text{Br}^-$ ,  $\text{SO}_4^{2-}$ ). In this work, the causal relationships by Köhler et al. were used to calculate composition specific LCI data for the treatment of aqueous wastes generated by the paracetamol process. As it was assumed that all aqueous waste streams would be mixed before treatment, the average wastewater properties of the combined aqueous process wastes were determined, which are given in Table S40.



Based on the average composition of the mixed aqueous waste leaving the paracetamol process (high in  $\text{TOC}_{\text{degradable}}$ , acidic PH), the likely sequence of required wastewater purification technologies was determined as mechanical-biological treatment followed by incineration of excess sludge. Mechanical-biological wastewater treatment was modelled assuming that the microbial decomposition of organic compounds and nitrogen species proceeds exclusively *via* aerobic degradation to  $\text{CO}_2$  and  $\text{H}_2\text{O}$ . Aerobic degradation reactions for all biodegradable compounds contained in the paracetamol process wastewater are listed in Table S41. A detailed account of the LCI calculations carried out to model the mechanical-biological wastewater treatment process can be found in SI Section S6.2.

Incineration of excess sludge is performed to mineralise poorly bio-degradable wastewater pollutants. To calculate a process inventory for sludge incineration, consumption and emission factors were used that quantify the mass of process-related material flows per mass of incinerated sludge (SI Section S6.3). The employed factors were adapted from Köhler,<sup>67</sup> and pertain to a sludge treatment facility comprising unit operations for sludge dewatering, incineration, flue gas purification and steam generation. When modelling sludge incineration for wastewater treatment of the paracetamol process, complete combustion of all excess sludge to  $\text{CO}_2$  and  $\text{H}_2\text{O}$  was assumed.

## 2.6 LCA goal and scope definition

LCA was performed for the conceptual design of a continuous, industrial-scale manufacture of crude paracetamol from bio-renewable CST waste *via*  $\beta$ -pinene. The goal of the study was to obtain initial LCIA estimates of the novel process, identify process hotspots to guide future research and provide a dataset for comparison against LCA results of other paracetamol production routes. Furthermore, the study aimed to compare the environmental impacts of obtaining CST-derived  $\beta$ -pinene feedstock to the impacts of obtaining benzene, a common feedstock for conventional paracetamol synthesis. The findings of this study benefit the progress of the pharmaceutical industry towards green chemistry, and provide well-documented datasets to the LCA and process engineering communities.

The scope of the study encompasses a cradle-to-gate system boundary around a simulated chemical plant that manufactures crude paracetamol from raw materials using CST-derived  $\beta$ -pinene, considering all material and energy flows associated with the process, but excluding the production of capital goods (Figure 3). The assessed manufacturing plant was modelled to be located in Europe in order to reduce transportation impacts through proximity to CST-producing Kraft pulping sites in Northern Europe as well as through proximity to the local European market, supporting the decentralisation of the pharmaceutical industry. As LCA studies of pharmaceuticals commonly reference environmental impacts to the mass of product output,<sup>68</sup> the functional unit for this study was defined as the production of one metric tonne of crude paracetamol, which is in line with the anticipated production scale of the future plant. Further processing of crude paracetamol (e.g., recrystallisation, tableting, packaging) was excluded from this study, as were the product's use and end-of-life stages. These steps are likely to resemble the life-cycle steps of conventional paracetamol manufacture; for LCAs on tableting and packaging of conventional paracetamol products the reader is referred elsewhere.<sup>69</sup>

The LCA model was built using GaBi ts software (v10.0.1.92)<sup>70</sup> with the ReCiPe 2016 v1.1 midpoint-level (H) impact assessment methodology. A description of the developed GaBi model is given in SI Section S7.1. Core LCI data for this study was extracted from a model of the manufacturing process constructed in Aspen using bench-scale experimental data. An LCI for CST production from Kraft pulping was adopted from the literature.<sup>17</sup> LCI data for ozone production was adopted from online manufacturer data as outlined in SI Section S3.2. Background LCI datasets for the manufacture of feedstock chemicals, energy provision and transportation were imported from ecoinvent<sup>71</sup> 3.7 and GaBi Professional databases, selecting European datasets where available. Table S49 lists the imported database LCI modules. To represent direct substance flows between the paracetamol process and the ecosphere in the GaBi model, pre-defined elementary flows for resources and emissions from ecoinvent and GaBi Professional were used, which are listed in Table S50.

It is acknowledged that, owing to the research state of the process, the available experimental data was of varied quality and completeness. Where necessary, simplifying assumptions and/or proxy data were used to develop the process models. Thus, the inventory data

employed in the LCA model involves a considerable degree of uncertainty, inevitably affecting the accuracy of the calculated LCA results. However, efforts to adopt conservative LCI estimates were made at all points of this study such that the final LCA results represent worst-case scenarios.

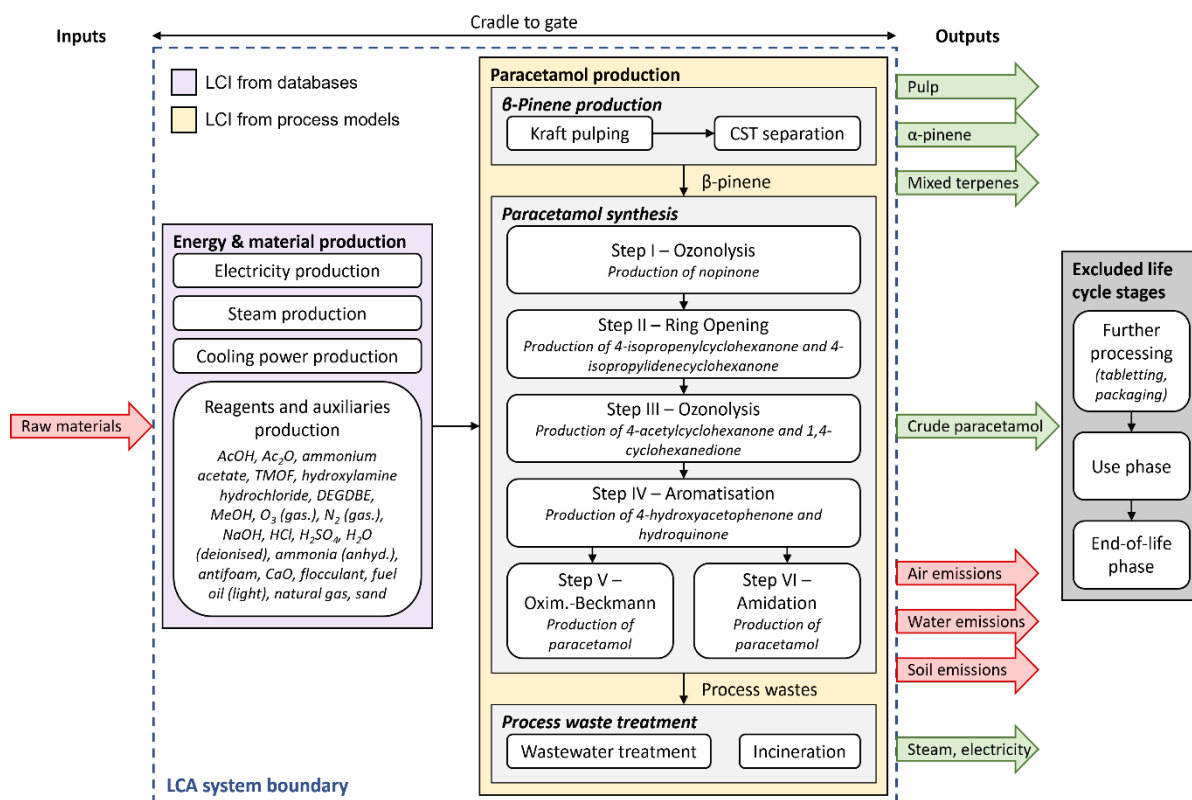


Figure 3. Cradle-to-gate system boundary (dashed blue line) employed for this LCA study, encompassing the manufacture of crude paracetamol API from raw materials using CST-derived  $\beta$ -pinene. The out-bound green arrows represent the system's products and co-products.

### 3. Results and Discussion

#### 3.1 Process model results

##### *Thermal separation of $\beta$ -pinene from CST*

The designed CST fractionation model includes two distillation columns for desulphurization, two for  $\alpha$ -pinene recovery and three for  $\beta$ -pinene recovery. A detailed process model description is provided in Section 2.3. Simulations of the fractionation train show successful separation of CST into sulphurous waste and three desulphurised terpene fractions (sulphurous compound contents < 5 ppm), including the  $\beta$ -pinene product stream (95 wt.%  $\beta$ -

pinene), an  $\alpha$ -pinene stream (95 wt.%  $\alpha$ -pinene), and a carene-dominant mixed terpene stream (69 wt.% carene). Further purification of the terpene streams was not modelled. Overall, the model shows that ~38.5 wt.% of  $\beta$ -pinene contained in the CST feed could be recovered into the  $\beta$ -pinene product stream.

Due to the proximity of the normal boiling points of terpenes (Table 2), sophisticated CST separation technologies such as a combination of vacuum fractionation and reactive distillation are likely to yield superior separation results at higher efficiency than ordinary distillation. However, such methods for CST separation could not be modelled accurately due to lack of available data. Ordinary distillation, on the other hand, could be modelled reliably based on VLE predictions only. It is expected that further experimental research into CST separation methods can yield more effective  $\beta$ -pinene isolation processes.

#### *Industrial manufacture of paracetamol from $\beta$ -pinene via process steps I – VI*

The manufacture of paracetamol from CST-derived  $\beta$ -pinene *via* six process steps (I – VI) was modelled in Aspen based on the experimental datasets summarised in Table S1. Detailed process model descriptions are given in Section 2.3 and SI Section S3.

The simulation results show that paracetamol could be attained from steps V and VI at purities of >99.9 wt.% and 98 wt.%, respectively. The molar yield of paracetamol from  $\beta$ -pinene across the entire process was predicted to be 47.6%, with roughly twice as much paracetamol yielded in step V compared to step VI (molar ratio 73:27). On a mass basis, the overall yield implies a feed-to-product ratio of 1.89, meaning 1.89 mass units of  $\beta$ -pinene are required per unit of paracetamol produced.

### **3.2 LCIs for $\beta$ -pinene isolation and paracetamol manufacture**

Gate-to-gate LCIs for the isolation of  $\beta$ -pinene from CST and for the manufacture of paracetamol from  $\beta$ -pinene were assembled using the Aspen process models of the proposed process, as no such inventories were publicly reported elsewhere at the time of this study.

The process flows associated with the isolation of  $\beta$ -pinene from CST were extracted from the CST fractionation model described in Sections 2.3 and 3.1. While the  $\beta$ -pinene product

obtained in the CST fractionation model has 95 wt.% purity, it is expected that the resource requirements of isolating pure  $\beta$ -pinene from CST are sufficiently represented. This is because other CST separation techniques, that could not be considered in this study due to data limitations, are expected to be more efficient than distillation, rendering the resource requirement predictions for CST separation from the fractionation model a likely overestimate of the actual resources required to isolate  $\beta$ -pinene from CST. The resulting process LCI for  $\beta$ -pinene isolation from CST is shown in Table 3.

The gate-to-gate LCI for the manufacture of paracetamol from  $\beta$ -pinene was extracted from the Aspen simulations of process steps I to VI, and supplemented with estimated resource requirements for the provision of ozone based on manufacturer's data (cf. SI Section S3.2). The resulting LCI summarising the calculated material inputs, energy requirements and emissions associated with paracetamol production from  $\beta$ -pinene feed is shown in Table 4.

Deconvoluted gate-to-gate LCI datasets for each process step (I – VI) are given in SI Section S4.2, Tables S29 – S34. These describe the predicted process flows associated with the manufacture of intermediates from each step, such as nopinone manufacture from  $\beta$ -pinene, or paracetamol production from 4-hydroxyacetophenone. As these datasets are more granular, they can be used during LCIA of the proposed paracetamol process to identify resource intensive process hotspots. Additionally, these datasets are useful to the wider LCA community as the obtained gate-to-gate LCI modules of each process step may be integrated into LCA studies of other chemical manufacturing routes, where appropriate.

The accuracy of the developed LCI datasets depends on the reliability of the constructed process models which, in turn, is a function of the experimental datasets used. As the datasets available for this study were of varied quality and completeness, the extracted LCIs for process steps I – VI bear inevitable uncertainties that cannot be quantified at this stage of process development without further experimental work. However, the authors are confident that the presented LCIs represent worst-case scenarios in terms of resource consumption and emissions.

Table 3. Gate-to-gate life cycle inventory for the isolation of  $\beta$ -pinene from CST *via* a distillation train.

| LCI: Isolation of $\beta$ -pinene from CST <i>via</i> distillation |                       |      |                                    |                       |      |
|--|-----------------------|------|------------------------------------|-----------------------|------|
| Inputs   | Value                 | Unit | Outputs                            | Value                 | Unit |
| <b>Material inputs</b>   |                       |      | <b>Material outputs</b>            |                       |      |
| CST  | 41.1                  | kg   | $\beta$ -pinene (liquid, 95 mol%)  | 1.00                  | kg   |
|  |                       |      | $\alpha$ -pinene                   | $1.64 \times 10^{-2}$ | kg   |
| <b>Utility inputs</b>  |                       |      | $\beta$ -pinene                    | $9.50 \times 10^{-1}$ | kg   |
| Electricity  | $8.57 \times 10^{-4}$ | kWh  | 3-carene                           | $3.37 \times 10^{-2}$ | kg   |
| Pump 1   | $6.57 \times 10^{-4}$ | kWh  | $\alpha$ -pinene (liquid, 97 mol%) | 23.3                  | kg   |
| Pump 2   | $2.00 \times 10^{-4}$ | kWh  | $\alpha$ -pinene                   | 22.7                  | kg   |
| Cooling (cooling water)  | 97.2                  | MJ   | $\beta$ -pinene                    | $3.75 \times 10^{-1}$ | kg   |
| Condenser – column 1   | 1.44                  | MJ   | 3-carene                           | $2.47 \times 10^{-1}$ | kg   |
| Condenser – column 2   | 8.99                  | MJ   | d-limonene                         | $2.55 \times 10^{-2}$ | kg   |
| Condenser – column 3   | 4.04                  | MJ   | 3-carene (liquid, 69 mol%)         | 11.5                  | kg   |
| Condenser – column 4   | 54.5                  | MJ   | $\beta$ -pinene                    | 1.13                  | kg   |
| Condenser – column 5   | 17.4                  | MJ   | 3-carene                           | 7.93                  | kg   |
| Condenser – column 6   | 6.53                  | MJ   | d-limonene                         | 2.44                  | kg   |
| Condenser – column 7   | 4.39                  | MJ   |                                    |                       |      |
| Heating (HP steam)   | 87.8                  | MJ   | <b>Utility outputs</b>             |                       |      |
| Reboiler – column 4  | 59.7                  | MJ   | n/a                                | -                     | -    |
| Reboiler – column 5  | 17.3                  | MJ   |                                    |                       |      |
| Reboiler – column 6  | 6.34                  | MJ   | <b>Direct emissions to air</b>     |                       |      |
| Reboiler – column 7  | 4.38                  | MJ   | n/a                                | -                     | -    |
| Preheater – column 7   | $1.13 \times 10^{-1}$ | MJ   |                                    |                       |      |
| Heating (MP steam)   | 27.2                  | MJ   | <b>Direct emissions to water</b>   |                       |      |
| Reboiler – column 1  | 5.44                  | MJ   | n/a                                | -                     | -    |
| Reboiler – column 2  | 10.4                  | MJ   |                                    |                       |      |
| Reboiler – column 3  | 2.95                  | MJ   | <b>Direct emissions to water</b>   |                       |      |
| Preheater – column 1   | 8.14                  | MJ   | n/a                                | -                     | -    |
| Preheater – column 6   | $2.92 \times 10^{-1}$ | MJ   |                                    |                       |      |
|  |                       |      | <b>Waste outputs</b>               |                       |      |
|  |                       |      | Waste, sulphurous organics         | 5.30                  | kg   |
|  |                       |      | dimethyl sulphide                  | 2.06                  | kg   |
|  |                       |      | dimethyl disulphide                | $2.06 \times 10^{-1}$ | kg   |
|  |                       |      | methyl mercaptan                   | 1.03                  | kg   |
|  |                       |      | $\alpha$ -pinene                   | 1.98                  | kg   |
|  |                       |      | $\beta$ -pinene                    | $1.44 \times 10^{-2}$ | kg   |
|  |                       |      | 3-carene                           | $1.61 \times 10^{-2}$ | kg   |

Table 4. Gate-to-gate life cycle inventory for the manufacture of paracetamol from  $\beta$ -pinene *via* process steps I – VI.

| LCI: Manufacture of paracetamol from $\beta$ -pinene |                       |      |                         |       |      |
|--|-----------------------|------|-------------------------|-------|------|
| Inputs   | Value                 | Unit | Outputs                 | Value | Unit |
| <b>Material inputs</b>                               |                       |      | <b>Material outputs</b> |       |      |
| Beta-pinene  | 1.89                  | kg   | Paracetamol (solid)     | 1.00  | kg   |
| Methanol   | 9.88                  | kg   |                         |       |      |
| Trimethyl orthoformate                               | 1.46                  | kg   | <b>Utility outputs</b>  |       |      |
| Diethylene glycol dibutyl                            | $5.03 \times 10^{-1}$ | kg   | n/a                     | -     | -    |

|                             |                      |     |  |                         |
|-----------------------------|----------------------|-----|--|-------------------------|
| ether                       |                      |     |  |                         |
| Acetic anhydride            | $2.77 \cdot 10^{-1}$ | kg  | <b>Direct emissions to air</b>                   |                         |
| Ammonium acetate            | $1.68 \cdot 10^{-1}$ | kg  | CO <sub>2</sub> (gaseous)                        | $1.55 \cdot 10^{-1}$ kg |
| Acetic acid                 | $8.72 \cdot 10^{-2}$ | kg  | H <sub>2</sub> O (gaseous)                       | $1.50 \cdot 10^{-3}$ kg |
| Sulphuric acid (98 wt.%)    | $2.82 \cdot 10^{-2}$ | kg  | N <sub>2</sub> (gaseous)                         | 10.5 kg                 |
| Hydrochloric acid (30 wt.%) | 1.78                 | kg  | <b>Direct emissions to water</b>                 |                         |
| Hydroxylamine hydrochloride | $3.76 \cdot 10^{-1}$ | kg  | n/a  | - -                     |
| Sodium hydroxide            | $5.86 \cdot 10^{-1}$ | kg  | <b>Direct emissions to water</b>                 |                         |
| Sodium carbonate            | $7.11 \cdot 10^{-1}$ | kg  | n/a  | - -                     |
| Water, deionised            | 23.9                 | kg  | <b>Waste outputs</b>                             |                         |
| Oxygen (gaseous)            | 23.8                 | kg  | Waste, mixed (gaseous)                           | 26.6 kg                 |
| Nitrogen (gaseous)          | 10.5                 | kg  | 84 wt.% O <sub>2</sub> , 4 wt.% O <sub>3</sub> , | 26.0 kg                 |
| <b>Utility inputs</b>       |                      |     | 11 wt.% mixed organics.                          |                         |
| Electricity                 | 22.0                 | kWh | 66 wt.% methyl formate,                          | $5.50 \cdot 10^{-1}$ kg |
| Cooling (cooling water)     | 120                  | MJ  | 27 wt.% mixed organics,                          |                         |
| Cooling (chilled water)     | 18.0                 | MJ  | 7 wt.% H <sub>2</sub> O.                         |                         |
| Cooling (refrigerant)       | 1.90                 | MJ  | Waste, aqueous (liquid)                          | 28.0 kg                 |
| Heating (HP steam)          | 93.7                 | MJ  | Halogenated                                      | 20.7 kg                 |
| Heating (MP steam)          | 18.0                 | MJ  | Non-halogenated                                  | 1.33 kg                 |
| Heating (LP steam)          | 3.08                 | MJ  | Non-halogenated, acidic                          | 5.99 kg                 |
|                             |                      |     | Waste, organic (liquid)                          | 8.61 kg                 |
|                             |                      |     | Waste, organic (solid)                           | $8.78 \cdot 10^{-1}$ kg |
|                             |                      |     | unspecified crystalline                          | $8.78 \cdot 10^{-1}$ kg |
|                             |                      |     | organics, MW 140-180                             |                         |

### 3.3 Waste generation and treatment; calculated LCIs

Several organic and aqueous waste streams are generated throughout the proposed manufacture of paracetamol from  $\beta$ -pinene, which must be adequately treated before they can be returned to the ecosphere or re-used within the technosphere.

Organic process wastes were found to mainly originate from process steps I, III, IV and VI, where organic solvents are used in significant quantities. Here, the use of waste purification and recycling strategies such as distillation, two-phase extraction or membrane separation is desirable to avoid the environmental burdens associated with the manufacture of virgin materials. As the generated organic wastes are non-halogenated and of low water content, the process may offer several opportunities for effective waste recovery. However, initial experimental work mainly focussed on the synthesis and separation of product molecules and only partially investigated the purification and reuse of waste streams, such as the recovery of acetic acid *via* distillation in step VI. Nonetheless, options for process-integrated recycling

of organic wastes were explored throughout all process steps using distillation and membrane separation models constructed in Aspen.

The developed models show that it is feasible to recycle at least 66.8% of methanol solvent fed to the reactor in step I, 74.7% of methanol in step III, 94.6% of DEGDBE solvent in step IV and 91.1% of acetic acid solvent in step VI (for process modelling details see SI Section S3). Notably, the estimated recycling rates represent conservative estimates as the composition complexity of the systems demanded use of large bleed streams in the absence of experimental data. Additionally, lack of experimental data made it impossible to reliably explore other sophisticated waste separation methods of potentially higher efficiency. Accordingly, the constructed process models estimate that 13.2 kg mixed organic waste per kg paracetamol produced could not be recycled within the modelled process and required disposal. Ideally, this waste should be exported for use in other process plants as low-grade solvents or feed streams. However, uncertainty regarding the extent and compositions of the organic waste streams made sales predictions at this early design stage impossible. Instead, it was assumed that all residual organic wastes needed to be eliminated *via* incineration. Organic waste incineration was modelled to take place in a thermal waste treatment plant with energy recovery. The developed model was based on a literature model of organic solvent incineration<sup>65</sup> and is described in Section 2.5. Using the constructed model an LCI for the incineration of organic process waste could be assembled, which is given in SI Section S5.4, Table S39.

The paracetamol process also creates considerable amounts of wastewater, including halogenated, acidic, and neutral waste streams. These wastewater streams mainly originate from process steps II, IV and V, where larger amounts of water are required for product separation. However, strategies for handling aqueous process wastes were not investigated experimentally. Instead, a model for the treatment and disposal of wastewater streams was constructed using a model for the treatment of industrial wastewaters from the literature.<sup>66,67</sup> In this context, it was determined that the mixed aqueous wastes leaving the novel paracetamol process likely require work-up through mechanical-biological wastewater treatment followed by incineration of generated biological sludge. The modelling of wastewater treatment strategies is described in Section 2.5. The predicted process flows



associated with the mechanical-biological treatment of aqueous process waste and with the incineration of excess biological sludge were summarised into wastewater treatment LCIs which are given in SI Section S6.4, Tables S47 and S48.

### **3.4 Plant capacity of the novel paracetamol manufacturing site**

To estimate a realistic plant capacity for the manufacture of paracetamol from CST-derived  $\beta$ -pinene several factors were considered. As outlined in the scope of this LCA study, the plant shall be situated in Europe for proximity to local Kraft pulping sites and the European pharmaceutical market. Based on figures published online, it was assumed that a non-integrated chemical pulp mill in Europe manufactures 800 000 t of pulp annually,<sup>72</sup> and that 1 kg CST is produced per 100 kg pulp.<sup>16</sup> Accordingly, it was estimated that 22 t of CST are generated per pulping site per day. Given that CST from Northern European softwood contains ~6 wt.%  $\beta$ -pinene (Table 2), and that 38.5 wt.% of the  $\beta$ -pinene contained in CST can be recovered into a purified  $\beta$ -pinene stream (Section 3.1), it was calculated that 0.5 t/day of purified  $\beta$ -pinene can be obtained from the CST supply of one Kraft pulping site. As the molar yield of crude paracetamol from purified  $\beta$ -pinene across the novel process was calculated as 47.6 mol% (Section 3.1), it was estimated that a paracetamol output of 0.26 t/day can be obtained from a paracetamol plant supplied by one Kraft pulping site. Notably, this represents a conservative estimate that is expected to increase significantly as the processes for  $\beta$ -pinene purification and paracetamol manufacture are optimised through further experimental work.

For this study, it was assumed that four European Kraft pulping sites are available to supply CST feed to the proposed process plant. As such, at the current level of process development, the realistically achievable production capacity of the novel process was predicted as 1 t/day paracetamol output. This production capacity is of the same order of magnitude as the lower end of conventional paracetamol plant outputs, which currently serve the global market.<sup>48–52</sup> Considering the novelty of the process and its overall aim to supply paracetamol to the local market, a paracetamol output of 1 t/day was deemed appropriate for the proposed paracetamol plant.

### 3.5 Comparative LCA of $\beta$ -pinene and benzene feedstock

The cradle-to-gate LCIA results of  $\beta$ -pinene and benzene feedstock production are shown in Figure 4 for the ReCiPe impact category 'Climate change'. The corresponding LCIA results for all other ReCiPe impact categories are given in SI Section S8.2, Table S52.

The results show that the environmental performance of  $\beta$ -pinene feedstock compared to benzene is strongly dependent on the method of allocation employed for the  $\beta$ -pinene production process. If the impacts of CST separation are entirely allocated to the  $\beta$ -pinene product stream (allocation scenario 1), then benzene outperforms  $\beta$ -pinene significantly across all LCIA categories, as reflected in columns 1 and 2 of Figure 4. However,  $\beta$ -pinene is arguably not the only product obtained from the CST separation system, as 43 kg of  $\alpha$ -pinene (95 wt.%) and 12 kg of desulphurised mixed terpenes (69 wt.% carene) are produced per kg of  $\beta$ -pinene. Consequentially, CST separation may be considered a multi-product system, where impacts are allocated amongst several system outputs, which yields a different and improved environmental performance result for  $\beta$ -pinene production from CST.

Two specific multi-product allocation scenarios were investigated. Firstly, the purified  $\alpha$ -pinene stream was considered equally valuable to the  $\beta$ -pinene product, and accordingly, the impacts of CST separation were allocated by mass to both streams (allocation scenario 2). For this scenario, LCIA results show that the environmental impacts of  $\beta$ -pinene production are comparable to those of benzene, which is reflected in columns 1 and 3 of Figure 4. Secondly, the  $\alpha$ -pinene,  $\beta$ -pinene and mixed terpene streams were considered as three equally valuable products, and thus the impacts of CST separation were allocated by mass to all three terpene streams (allocation scenario 3). Here, LCIA results show that the environmental impacts of  $\beta$ -pinene production are significantly lower than those of benzene, as reflected in columns 1 and 4 of Figure 4. A detailed description of the employed allocation strategies is given in SI Section S8.1. Thus, the presented LCIA results confirm that  $\beta$ -pinene obtained from the investigated technologies for CST production and separation incurs fewer environmental impacts than benzene production if economically equivalent valorisation opportunities can be established for all three terpene product streams.

As allocation can be a controversial aspect of the LCA methodology due to its partially subjective nature, careful consideration is required when deciding which of the investigated allocation scenarios is most justifiable. Currently, all three terpene streams of interest are of similar economic value, as both pure and mixed desulphurised monoterpenes are widely used in lower value applications such as industrial solvents,<sup>73,74</sup> adhesive resins,<sup>75</sup> insecticides<sup>76</sup> and fragrance and flavouring agents.<sup>77,78</sup> Given that there is significant research into valorisation of both purified and mixed monoterpene streams for higher value applications, including their use as therapeutic agents<sup>79,80</sup> or as feedstock for fine chemicals production,<sup>31,34,35,79</sup> it is likely that the economic value of the different terpene product streams also remains comparable in magnitude in the future. Additionally, these research efforts suggest that various monoterpene sources may be able to substitute benzene and other petrochemical-derived feedstocks used in specialty chemicals production in the future. It was thus judged as likely that mass-based allocation of CST separation impacts to all three monoterpene product streams is justifiable for future applications.

Another noteworthy aspect of the LCIA results shown in Figure 4 and Table S52 is that the calculated impacts for CST-derived  $\beta$ -pinene production most certainly are overestimates. From Figure 4 it is evident that the main share of impacts for  $\beta$ -pinene production stems from the CST separation process. As the CST separation technology employed for this study was fractional distillation, the associated impacts are expected to reduce significantly upon plant-wide heat integration which, at this stage of process development, was not yet considered. Additionally, while fractional distillation was practical to model during early-stage process development, it is not necessarily the most efficient methodology for CST separation due to the monoterpene's proximity in boiling points. Here, collecting data to investigate other technologies for CST separation, such as reactive distillation, has large potential to bring significant impact reductions for the  $\beta$ -pinene production process. This stands in stark contrast to the LCIA results obtained for benzene production, which are derived from the well-established process for benzene manufacture *via* catalytic reforming of crude oil, and are thus unlikely to represent an overestimate. Therefore, it is anticipated that bio-renewable  $\beta$ -pinene feedstock obtained from a fully developed CST separation process will incur equal or lower environmental impacts than benzene production, irrespective of the allocation strategy chosen.

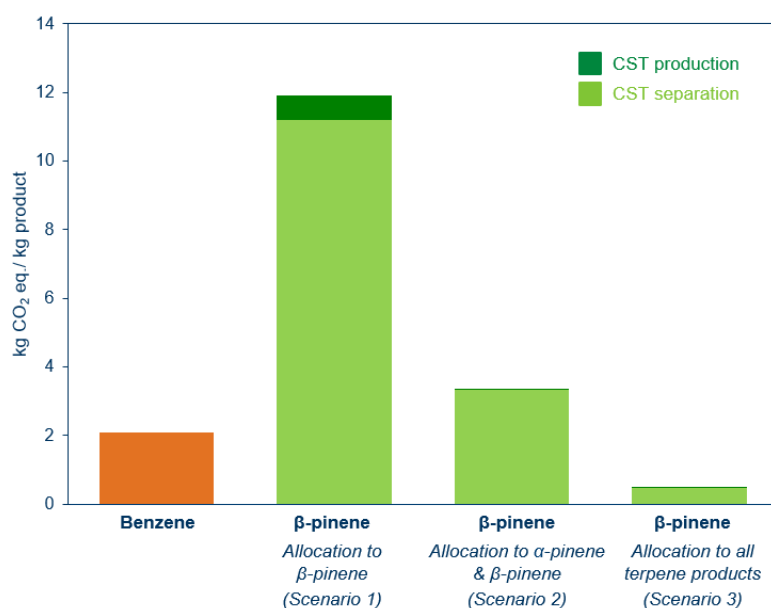


Figure 4. LCIA results from the cradle-to-gate LCA of benzene and  $\beta$ -pinene feedstock production, respectively, for the ReCiPe 2016 v1.1 midpoint-level (H) impact category 'Climate change'.

### 3.6 LCIA results of the novel paracetamol production process

The cradle-to-gate LCIA results of the proposed paracetamol production process are shown in Figure 5 for selected ReCiPe impact categories. A full list of the calculated LCIA results for all ReCiPe impact categories is given in SI Section S8.3, Table S53.

To understand the significance of the calculated LCIA values, the obtained impact results should be compared to cradle-to-gate impacts of conventional paracetamol manufacturing processes. Unfortunately, corresponding LCA studies for conventional paracetamol production are currently not publicly accessible, and thus a scrutinizing comparison between the proposed bio-based paracetamol process and conventional petrochemical-based production could not be included in this study. However, future comparative assessments employing the LCIA values presented in this study must acknowledge that paracetamol production based on  $\beta$ -pinene as presented herein is far from optimised due to the early-design-stage nature of the project, and thus the associated LCIA results represent a worst-case scenario in terms of environmental impacts incurred per tonne of paracetamol produced.

Figure 5 and Table S53 highlight the contributions of  $\beta$ -pinene production, paracetamol manufacture (process steps I – VI) and waste disposal to the overall cradle-to-gate impact result for each ReCiPe category. Interestingly, the impacts of waste disposal and their effects on the overall LCIA results were found to vary vastly between different impact categories. This is because the employed waste treatment procedures include waste-to-energy incineration processes that produce electricity and steam, which grant environmental credits to the waste disposal process due to avoided burdens of producing these energy carriers otherwise. These credits incur a net environmental benefit for waste disposal in 3 out of 19 ReCiPe impact categories, and strongly influence the overall LCIA results of the paracetamol production process. However, while waste hierarchies generally favour waste-to-energy strategies over landfilling, further process development will aim to substitute incineration with superior strategies, which were not explored in this study due to the early-design-stage data limitations. This means that the LCIA results for waste disposal may see an apparent increase in environmental impacts upon waste treatment optimisation due to a reduction in waste-to-energy derived credits. However, losses in credits would be compensated for by fewer impacts incurred from waste disposal due to reduced waste volumes, as well as by fewer impacts attributed to paracetamol production due to reduced resource consumption. Thus, the overall environmental performance of the novel process is likely to improve upon further implementation of reuse and recycling strategies despite a loss in waste-to-energy derived credits.

The most significant contributions to the overall environmental impacts of the proposed process were found to stem from the manufacture of paracetamol from  $\beta$ -pinene. Figure 5 and Table S53 show that the impacts associated with paracetamol manufacture are much larger than the impacts of  $\beta$ -pinene feedstock production across all impact categories. This is unsurprising, as significantly more processing steps are involved in paracetamol manufacture from  $\beta$ -pinene than in  $\beta$ -pinene production from CST. To understand what aspects of paracetamol manufacture from  $\beta$ -pinene incur the most impacts such that future process optimisation can effectively target environmental process hotspots, an in-depth hotspot analysis of process steps I – VI was carried out.

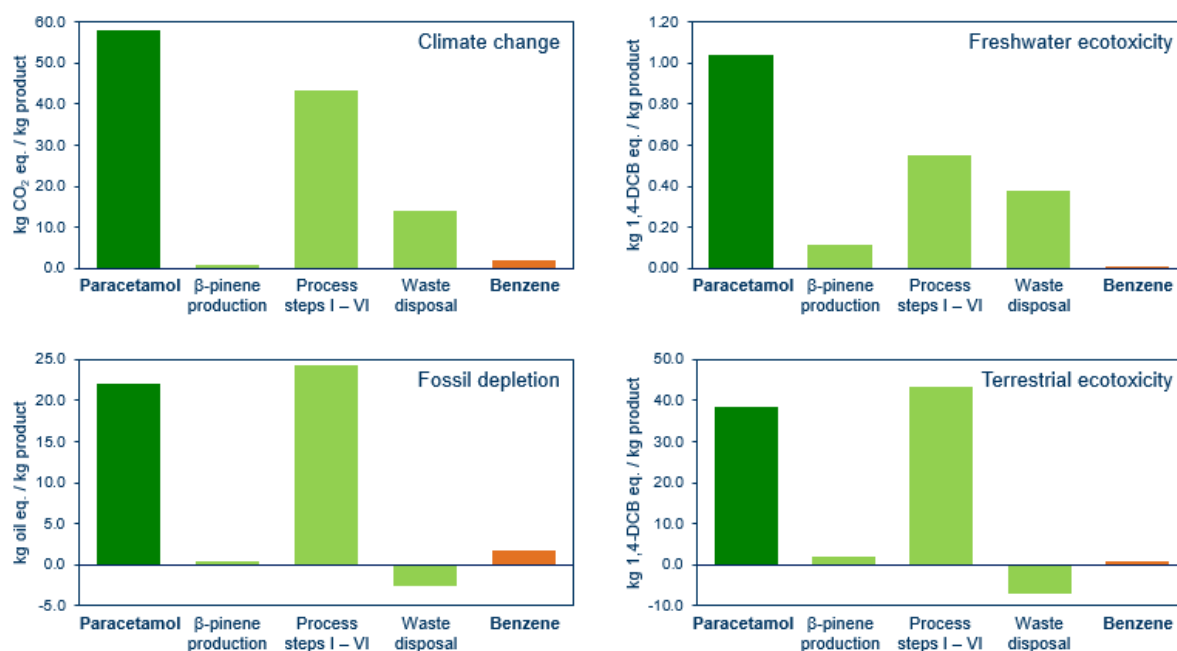


Figure 5. LCIA results of cradle-to-gate paracetamol production *via* the proposed process for the ReCiPe 2016 v1.1 midpoint-level (H) categories ‘Climate change’, ‘Freshwater ecotoxicity’, ‘Fossil depletion’ and ‘Terrestrial ecotoxicity’. The figure highlights the contributions of  $\beta$ -pinene feedstock production, paracetamol manufacture (process steps I – VI) and waste disposal (all light green) to the total impacts of paracetamol production (dark green). The impacts of benzene production are shown as a comparative benchmark value.

### 3.7 Process hotspots in the manufacture of paracetamol from $\beta$ -pinene

Based on the LCIA results presented above, optimisation of paracetamol manufacture from  $\beta$ -pinene holds significant potential to further reduce the environmental impacts of the new process. Here, early-design-stage hotspot analysis is a useful tool to promote effective and economical process optimisation, as it allows to identify resource-intensive process hotspots early on.

In this study, a hotspot analysis was carried out to evaluate the relative contributions of process steps I – VI to the environmental impacts of paracetamol production, such that the process steps with the largest impact contributions could be detected. The analysis was based on the cradle-to-gate impacts incurred by each process step per kg paracetamol production, and focussed on impacts arising from the resource consumption of each process step. Importantly, impacts incurred from the production of each step’s main substrate were not

included in the impacts attributed to that step, as these production impacts are already accounted for in the respective previous process step and should not be double counted. The results of the conducted hotspot analysis are shown in Figure 6.

The hotspot analysis showed that, except for process step VI, each process step exhibits large impact contributions in at least one category. However, from the heatmap in Figure 6b it is evident that steps I and III incur the overall greatest impact contributions to paracetamol production at the current state of process development, followed by process step IV. This suggests that further process optimisation should focus on process steps I, III and IV, as these hold the highest potential for significant impact reductions upon process improvement.

It is unsurprising that process steps I and III show similar impact contributions to the overall LCIA results, as both these steps involve ozonolysis reactions and feature the same reaction and separation technologies. To provide systematic guidance for the optimisation of individual process steps, the key impact contributing activities within steps I – VI were determined within a more granular hotspot analysis. The results presented in Figure 7 show the relative impact contributions of the main operational activities within steps I and IV; results for the remaining process steps are shown in SI Section S8.4.

The results shown in Figure 7 reveal that the key impact contributing activities within process step I are the consumption of ozone reagent and the use of methanol solvent. Therefore, the reduction of ozone and methanol consumption in step I represent important tasks for impactful process optimisation. In this study, ozone reagent was fed at 87% excess to the ozonolysis reactor, as initial experiments showed that product yield was lower for near-stoichiometric ozone feed and plateaued for larger ozone supply at the tested operating conditions. By investigating yet unexplored ranges between near-stoichiometric and 87% excess ozone feed, and by fine-tuning residence time and other operating parameters, further research should reduce the overall ozone consumption without loss in product yield. Methanol-water solvent (95:5 v/v) is used in large quantities during ozonolysis to dilute the reaction feed and aid in temperature control of the exothermic reaction. Accordingly, step I methanol consumption may be reduced by investigations to increase the solvent water content without compromising reaction performance. Additionally, 33.2% of spent methanol

solvent is discarded rather than recycled in the current process model to avoid accumulation of by-products in the recycling loop. Here, methanol consumption may feasibly be reduced by further research on the formation and behaviour by-products in process step I, as this will allow to optimise the methanol recycling strategy.

For process step IV, Figure 7 indicates that the consumption of utilities is the key contributing factor to the overall environmental impacts. More specifically, the majority of environmental impacts in this step were found to stem from the consumption of steam required to pre-heat the feeds to the multi-stage aromatisation reactor. This suggests that implementing a plant-wide heat integration strategy will pay off highly in reducing the environmental impacts incurred from process step IV.

To identify impactful process optimisation opportunities within the remaining process steps, similar analyses as described above for process steps I and IV may be carried out using the hotspot plots shown in SI Section S8.4, in combination with the detailed process model descriptions provided in SI Section S3.

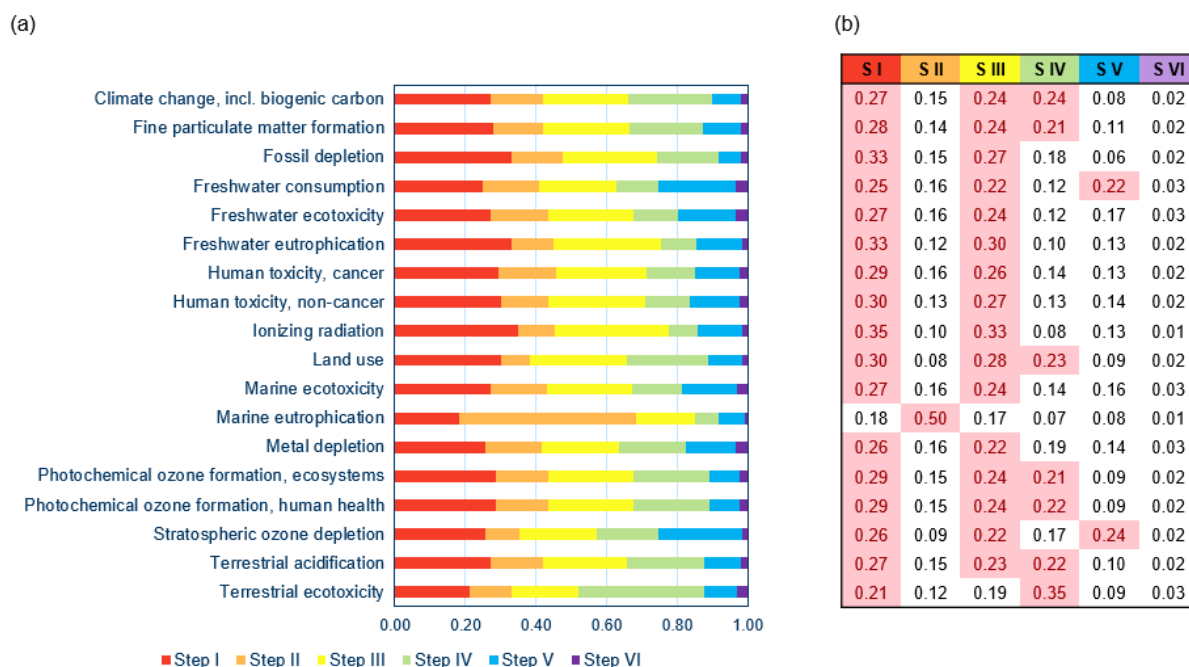


Figure 6. Hotspot analysis results showing the contributions of individual processing steps (S I – S VI) to the environmental impacts of paracetamol manufacture from  $\beta$ -pinene *via* the novel process.



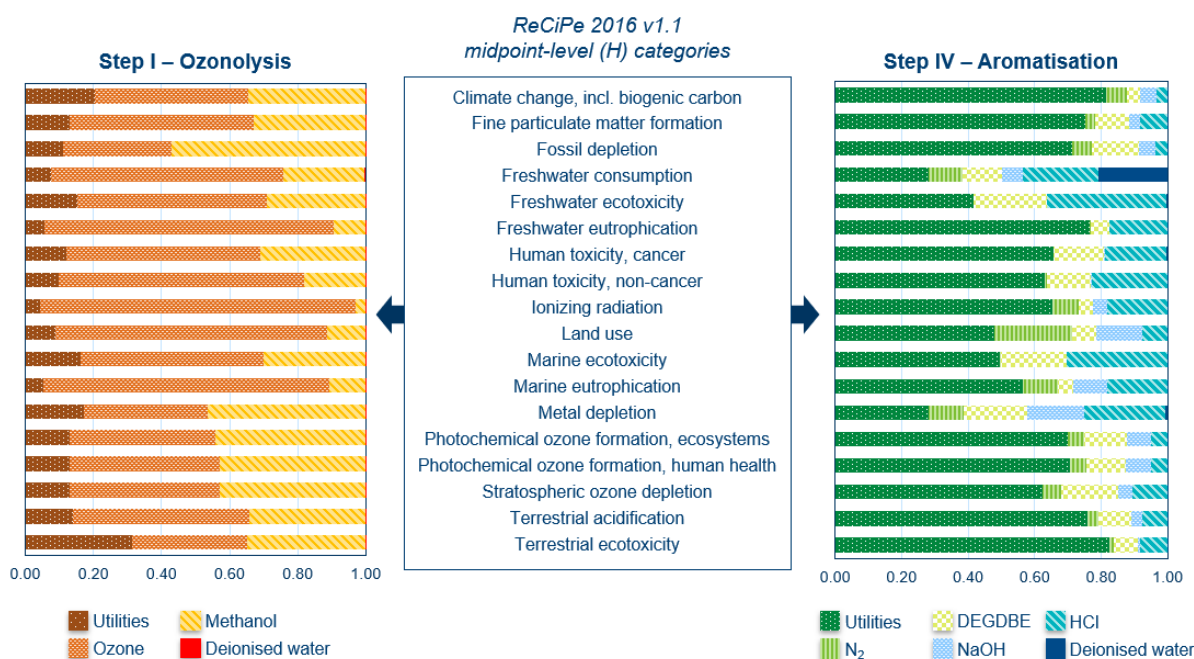


Figure 7. Stacked bar chart showing the relative contributions of the main operational activities within process steps I and IV to each impact category of the ReCiPe 2016 v1.1 midpoint-level (H) impact assessment methodology, allowing to identify key process hotspots.

#### 4. Conclusions

Environmental, societal, and economic challenges are driving the development of decentralised biorefineries. However, bio-based production must feature green chemistry and high process efficiency in addition to renewable feedstocks in order to achieve long-term process sustainability. This is particularly true as biorefineries commonly involve more complex reaction and separation procedures than petrochemical-based processes. Thus, a challenging but crucial task in the development of industrial biorefineries is the identification and elimination of resource-intensive process hotspots at the early-design stage.

In this study, we presented complete process models for the continuous, industrial-scale manufacture of paracetamol *via* a novel synthesis route that uses CST-derived  $\beta$ -pinene feed. To obtain reliable models despite the process' early design stage, conservative estimates were adopted when gaps in available experimental data were encountered. The developed Aspen Plus models predicted a 47.6 mol% paracetamol yield from  $\beta$ -pinene at 98 wt.% – 99.9 wt.% product purity. Furthermore, a VLE-based CST separation model predicted that at least 38.5% of the  $\beta$ -pinene contained in CST can be recovered into a desulphurised  $\beta$ -pinene stream, with yield improvements expected upon experimental investigation of other CST separation techniques. Future work to eliminate model uncertainties should focus on the experimental identification of side and by-products. Proxy literature models had to be used to model waste treatment processes, as primary experimental data for waste treatment is generally not collected during early research. In this respect, the shortage of available tools to predict process flows associated with the treatment of non-recyclable process wastes was identified as a key challenge for rigorous LCI assembly at the early design stage.

The calculated material and energy flows across the proposed process were summarised into gated LCIs. From the process models, a realistic plant capacity for  $\beta$ -pinene-based paracetamol manufacture using locally sourced CST in a European plant was estimated as 1 tonne/day. The environmental impacts associated with this process were quantified *via* cradle-to-gate LCA, and worst-case-scenario LCIA results were obtained that are expected to improve with further process development. This must be acknowledged when benchmarking against LCAs of conventional paracetamol manufacture, which were not available at the time of this study. The obtained LCIA results were used to assess feedstock sustainability, and we showed that

CST-derived  $\beta$ -pinene constitutes a greener feedstock than benzene if and when CST separation can be considered a multi-product system with mass-based impact allocation. To effectively guide future process development, we also used the LCIA results to conduct a process hotspot analysis, in which process steps I, III and IV were identified as the most resource-intensive process sections.

### Supporting materials

Three files were submitted as supporting materials alongside this manuscript.

File 1 – *Supporting Information*. This file contains process model descriptions and LCA results:

- S1 Summarised bench-scale experimental data of paracetamol synthesis from  $\beta$ -pinene
- S2 Description of the property estimation set-up for the developed Aspen Plus process models (thermodynamic modelling, proxy values for non-databank model parameters, user-supplied pure-component property data)
- S3 Verbal descriptions of the developed Aspen Plus process models
- S4 Gate-to-gate LCI datasets for process steps I – VI
- S5 Description of LCI calculation for organic process waste treatment
- S6 Description of LCI calculation for aqueous process waste treatment
- S7 Description of LCA modelling in GaBi software
- S8 LCIA results of the investigated case study (allocation, numerical LCIA results, hotspot analysis graphs)

File 2 – *Supplementary Data*. This file contains unpublished experimental data that was used to model the life cycle impacts:

- Experimental data on the continuous flow ozonolysis of  $\beta$ -pinene towards nopinone
- Experimental data on the ring opening of nopinone in continuous flow
- Experimental data on the aromatisation of 1,4-cyclohexanedione and 4-acetylcyclohexanone / 4-methylcyclohexanone over a 10 wt.% Pd/C catalyst
- MEng Research Project report that supplied background experimental data on the conversion of 4-hydroxyacetophenone to paracetamol.

### Conflicts of Interest

The authors declare no conflicts of interest.

### **Acknowledgements**

SH gratefully acknowledges the Department of Chemical Engineering and Biotechnology at the University of Cambridge for the funding of her PhD studentship. VU thanks RWTH Aachen University and the ERASMUS + program for the scholarship supporting her exchange program at the University of Cambridge. This project was co-funded by the UKRI project “Terpene-based Manufacturing for Sustainable Chemical Feedstocks” EP/K014889. The authors are particularly grateful to Dr Sameer Khare, Dr Muhammad Arsalan Ashraf and Dr Pawel Plucinski for providing the chemical synthesis data that was used as a foundation for the analyses carried out in this paper. The authors are also thankful to Joshua Tibbetts from the University of Bath for providing a supply of synthesised nopinone for use in experiments. The authors would like to thank Dr Simon Sung, Dr Polina Yaseneva, Dr Connor Taylor, Dr Magda Barecka and Dr Parminder Kaur Aulakh for providing expert advice on various aspects of the presented work.

### **Author contributions**

The authors confirm contribution to this article as follows:

SH: Methodology, Validation, Investigation, Data Curation, Writing – Original Draft, Visualisation, Project Administration.

VU: Methodology, Investigation, Data Curation, Writing – Review & Editing.

AL: Conceptualisation, Resources, Writing – Review & Editing, Supervision, Project Administration, Funding Acquisition.

All authors reviewed the results and approved the final version of the manuscript.

### **Availability of Data**

The data that supports the findings of this study are available in the supporting materials of this article. Additional raw data employed for the construction of process models will be made available from the corresponding author upon reasonable request.

### **References**

1. European Commission & Directorate-General for Research and Innovation. *Innovating for sustainable growth: a bioeconomy for Europe*. (Publications Office, 2012).

doi:10.2777/6462

2. European Commission & Directorate-General for Research and Innovation. *A sustainable bioeconomy for Europe : strengthening the connection between economy, society and the environment : updated bioeconomy strategy*. (Publications Office, 2018). doi:10.2777/792130
3. Attard, T. M., Clark, J. H. & McElroy, C. R. Recent developments in key biorefinery areas. *Current Opinion in Green and Sustainable Chemistry* **21**, 64–74 (2020).
4. Buisman, G. J. H. & Lange, J. H. M. Arizona Chemical: Refining and Upgrading of Bio-Based and Renewable Feedstocks. in *Industrial Biorenewables: A Practical Viewpoint* 21–62 (2016). doi:10.1002/9781118843796.ch2
5. Christensen, C. H., Rass-Hansen, J., Marsden, C. C., Taarning, E. & Egeblad, K. The Renewable Chemicals Industry. *ChemSusChem* **1**, 283–289 (2008).
6. U.S. Energy Information Administration. Spot Prices for Crude Oil and Petroleum Products - Release Date 3rd Aug 2022. *U.A. Energy Information Administration* (2022). Available at: [https://www.eia.gov/dnav/pet/PET\\_PRI\\_SPT\\_S1\\_M.htm](https://www.eia.gov/dnav/pet/PET_PRI_SPT_S1_M.htm). (Accessed: 4th August 2022)
7. Clews, R. J. Upstream Oil and Gas. in *Project Finance for the International Petroleum Industry* 101–117 (Academic Press, an imprint of Elsevier, 2016). doi:10.1016/b978-0-12-800158-5.00006-2
8. Sheldon, R. A. Utilisation of biomass for sustainable fuels and chemicals: Molecules, methods and metrics. *Catal. Today* **167**, 3–13 (2011).
9. European Commission. The European Green Deal. **COM 640**, 1–24 (2019).
10. European Commission. Communication from the Commission: A New Industrial Strategy for Europe. **COM 102**, 1–17 (2020).
11. European Commission. Updating the 2020 New Industrial Strategy: Building a stronger Single Market for Europe’s recovery. **COM 350**, 1–22 (2021).
12. United Nations. Transforming Our World: the 2030 Agenda for Sustainable Development United Nations United Nations Transforming Our World: the 2030 Agenda for Sustainable Development. **A/RES/70/1**, 1–41 (2015).
13. SJÖSTRÖM, E. Wood-based Chemicals and Pulping by-products. In *Wood Chemistry* 225–248 (Academic Press, 1993). doi:10.1016/b978-0-08-092589-9.50014-0
14. Silvestre, A. J. D. & Gandini, A. Terpenes: Major sources, properties and applications. in *Monomers, Polymers and Composites from Renewable Resources* 17–38 (Elsevier, 2008). doi:10.1016/B978-0-08-045316-3.00002-8
15. Bolonio, D. *et al.* Techno-economic, Life Cycle, and Environmental Cost Assessment, of biojet fuel obtained from Pinus pinaster by turpentine hydrogenation. *Sustain. Energy Fuels* **6**, 2478–2489 (2022).
16. Alén, R. Pulp Mills and Wood-Based Biorefineries. in *Industrial Biorefineries and White Biotechnology* 91–126 (Elsevier, 2015). doi:10.1016/B978-0-444-63453-5.00003-3
17. Helmdach, D., Yaseneva, P., Heer, P. K., Schweidtmann, A. M. & Lapkin, A. A. A

- Multiobjective Optimization Including Results of Life Cycle Assessment in Developing Biorenewables-Based Processes. *ChemSusChem* **10**, 3632–3643 (2017).
18. Statista. Price of benzene worldwide from 2017 to 2022. *Statista.com* (2022). Available at: <https://www.statista.com/statistics/1171072/price-benzene-forecast-globally/>. (Accessed: 5th August 2022)
  19. Moore, Z. US August benzene contracts settle lower, tracking spot prices. *ICIS.com* (2017). Available at: <https://www.icis.com/explore/resources/news/2017/07/31/10129098/us-august-benzene-contracts-settle-lower-tracking-spot-prices/>. (Accessed: 5th August 2022)
  20. Moore, Z. US February benzene settles lower, market moves back into contango. *ICIS.com* (2018). Available at: <https://www.icis.com/explore/resources/news/2018/01/31/10188914/us-february-benzene-settles-lower-market-moves-back-into-contango/>. (Accessed: 5th August 2022)
  21. Moore, Z. US spot benzene reaches record highs on tight supply, improved demand. *ICIS.com* (2022). Available at: <https://www.icis.com/explore/resources/news/2022/06/17/10776377/us-spot-benzene-reaches-record-highs-on-tight-supply-improved-demand/?fbclid=IwAR2ETgcLtDw4s7HK3etnv7dOBcqiCAOJ-sDI9ANVWuG0g-P4U9u1Kq4o3jc>. (Accessed: 5th August 2022)
  22. ChemAnalyst. Benzene Price Trend and Forecast. (2022). Available at: <https://www.chemanalyst.com/Pricing-data/benzene-25>. (Accessed: 5th August 2022)
  23. Kavakka, J. & Torssell, S. Method for desulfurization of crude sulfate turpentine. WIPO Patent No. WO 2020/012328 A1. 1–27 (2020).
  24. Sinhmar, P. S. & Gogate, P. R. Ultra-deep desulfurization of crude sulfated turpentine using oxidation, adsorption and novel combination approach. *Environ. Technol. Innov.* **18**, 100682 (2020).
  25. Inomata, M. & Hanabusa, K. Purification of turpentine by a process for the recovery of one or more dissolved products from complex liquid mixtures. U.S. Patent No. US 3,857,902 A. 1–5 (1974).
  26. Izmet'ev, E. S., Rubtsova, S. & Kutchin, A. V. Environmental aspects of sulfate turpentine refining (review). *Theor. Appl. Ecol.* **2019**, 12–22 (2019).
  27. Höfer, R. The Pine Biorefinery Platform Chemicals Value Chain. in *Industrial Biorefineries and White Biotechnology* 127–155 (Elsevier, 2015). doi:10.1016/B978-0-444-63453-5.00004-5
  28. Knuutila, P. Wood sulphate turpentine as a gasoline bio-component. *Fuel* **104**, 101–108 (2013).
  29. Sell, C. Ingredients for the modern perfumery industry. in *The Chemistry of Fragrances* 52–131 (2007). doi:10.1039/9781847555342-00052
  30. Vespermann, K. A. C. *et al.* Biotransformation of  $\alpha$ - and  $\beta$ -pinene into flavor compounds. *Applied Microbiology and Biotechnology* **101**, 1805–1817 (2017).

31. Tibbetts, J. D. & Bull, S. D. Dimethyl sulfide facilitates acid catalysed ring opening of the bicyclic monoterpenes in crude sulfate turpentine to afford: p-menthadienes in good yield. *Green Chem.* **23**, 597–610 (2021).
32. Tibbetts, J. D. & Bull, S. D. p-Menthadienes as Biorenewable Feedstocks for a Monoterpene-Based Biorefinery. *Adv. Sustain. Syst.* **5**, 2000292 (2021).
33. Tibbetts, J. D., Russo, D., Lapkin, A. A. & Bull, S. D. Efficient Syntheses of Biobased Terephthalic Acid, p-Toluic Acid, and p-Methylacetophenone via One-Pot Catalytic Aerobic Oxidation of Monoterpene Derived Bio- p-cymene. *ACS Sustain. Chem. Eng.* (2021). doi:10.1021/acssuschemeng.1c02605
34. Cunningham, W. B. *et al.* Sustainable catalytic protocols for the solvent free epoxidation and: Anti -dihydroxylation of the alkene bonds of biorenewable terpene feedstocks using H<sub>2</sub>O<sub>2</sub> as oxidant. *Green Chem.* **22**, 513–524 (2020).
35. Fomenko, V. V., Laev, S. S. & Salakhutdinov, N. F. Catalytic epoxidation of 3-carene and limonene with aqueous hydrogen peroxide, and selective synthesis of  $\alpha$ -pinene epoxide from turpentine. *Catalysts* **11**, 436 (2021).
36. Ravasio, N., Zaccheria, F., Guidotti, M. & Psaro, R. Mono- and bifunctional heterogeneous catalytic transformation of terpenes and terpenoids. *Top. Catal.* **27**, 157–168 (2004).
37. Amin, M. & Iqbal, M. S. Solvent free synthesis of acetaminophen. U.S. Patent No. US 9,006,488 B1. (2015).
38. Joncour, R., Duguet, N., Méta y, E., Ferreira, A. & Lemaire, M. Amidation of phenol derivatives: A direct synthesis of paracetamol (acetaminophen) from hydroquinone. *Green Chem.* **16**, 2997–3002 (2014).
39. Schulman, H. L., Baron, F. A. & Weinberg, A. E. Preparation of N-acetyl-p-aminophenol. U.S. Patent No. US 3,917,695 A. (1975).
40. Benner, R. G. Process for preparing aminophenol. U.S. Patent No. 3,383,416 A. (1968).
41. Huber, J. J. & Mahwah, N. J. Stepwise reduction of p-nitrophenol. U.S. Patent No. 4,264,525 A. (1981).
42. Holtzclaw, C. R. & Bryan, W. J. Method of preparing para-aminophenol. U.S. Patent No. 3,177,256 A. (1965).
43. Fritch, J. R., Fruchey, O. S. & Horlenko, T. Production of acetaminophen. U.S. Patent No. US 4,954,652. (1988).
44. Davenport, K. & Hilton, C. Process for producing N-acyl-hydroxy aromatic amines. U.S. Patent No. US 4,524,217. (1985).
45. Fruscella, W. Benzene. in *Kirk-Othmer Encyclopedia of Chemical Technology* (John Wiley & Sons, Inc., 2002). doi:10.1002/0471238961.0205142606182119.a01.pub2
46. World Resources Institute & World Business Council for Sustainable Development. Corporate Value Chain (Scope 3) Accounting and Reporting Standard – Supplement to the GHG Protocol Corporate Accounting and Reporting Standard. *Greenhouse Gas Protocol* (2011).

47. European Commission. Pharmaceutical Strategy for Europe. **COM 761**, 1–25 (2020).
48. Grumiller, J., Grohs, H. & Reiner, C. “Increasing the resilience and security of supply of production post-COVID-19” - *The Case of Medical and Pharmaceutical Products*. (216). (2021).
49. Products. *Anqiu Lu’an Pharmaceutical Co., Ltd.* Available at: <http://www.luanpharm.com/english/cpml.asp>. (Accessed: 6th September 2022)
50. Paracetamol | Full range and Applications. *SEQENS SAS* Available at: <https://www.seqens.com/en/products/paracetamol/>. (Accessed: 6th September 2022)
51. Our Facilities. *Granules India Ltd.* Available at: <https://granulesindia.com/about-us/our-facilities/>. (Accessed: 6th September 2022)
52. API Paracetamol Facilities. *Farmson Pharmaceutical Gujarat Pvt. Ltd.* (2022). Available at: <https://www.farmson.com/infrastructure.html>. (Accessed: 6th September 2022)
53. Macdonald, G. Europe’s last paracetamol plant closes its doors. (2009). Available at: <https://www.outsourcing-pharma.com/Article/2009/01/06/Europe-s-last-paracetamol-plant-closes-its-doors>. (Accessed: 30th August 2020)
54. SEQENS SAS. France Relance program: SEQENS new paracetamol production unit. *Seqens Press Release* (2021). Available at: <https://www.seqens.com/en/with-the-support-of-the-france-relance-programme-and-in-partnership-with-sanofi-and-upsa-seqens-has-officially-launched-the-project-to-build-a-new-paracetamol-production-unit/>. (Accessed: 6th September 2022)
55. ISO. *Environmental management -- Life cycle assessment -- Principles and framework*. (ISO no. 14040, 2006).
56. ISO. *Environmental management -- Life cycle assessment -- Requirements and guidelines*. (ISO no. 14044, 2006).
57. Carlson, E. C. Don’t gamble with physical properties for simulations. *Chem. Eng. Prog.* **92**, 35–46 (1996).
58. Suppes, G. Selecting Thermodynamic Models for Process Simulation of Organic VLE and LLE Systems. 1–5 (2008). Available at: <https://pdfs.semanticscholar.org/d02d/3efae030db68a249bad67c684a635e565e3.pdf>. (Accessed: 30th July 2020)
59. Walas, S. M. 4 - Activity Coefficients. in *4 - Activity Coefficients; Phase Equilibria in Chemical Engineering* (ed. Walas, S. M.) 165–244 (Butterworth-Heinemann, 1985). doi:<https://doi.org/10.1016/B978-0-409-95162-2.50012-9>.
60. Aspen Technology Inc. *Aspen Plus V10 Help*. (2017).
61. Voutsas, E. C. & Tassios, D. P. Prediction of Infinite-Dilution Activity Coefficients in Binary Mixtures with UNIFAC. A Critical Evaluation. *Industrial and Engineering Chemistry Research* **35**, 1438–1445 (1996).
62. Lin, Y. *et al.* Comparison of activity coefficient models for electrolyte systems. *AIChE J.* **56**, 1334–1351 (2010).
63. Luyben, W. L. Effect of tray pressure drop on the trade-off between trays and energy.



- in *Industrial and Engineering Chemistry Research* **51**, 9186–9190 (American Chemical Society, 2012).
64. Rützel, P. I. L., Griffiths, J., Xiong, F. & Barratt, P. Ozone - technical aspects of its generation and use, Knowledge Paper No.3. *Air Products and Chemicals Inc.* (1999).
  65. Seyler, C., Hofstetter, T. B. & Hungerbühler, K. Life cycle inventory for thermal treatment of waste solvent from chemical industry: A multi-input allocation model. *J. Clean. Prod.* **13**, 1211–1224 (2005).
  66. Köhler, A., Hellweg, S., Recan, E. & Hungerbühler, K. Input-dependent life-cycle inventory model of industrial wastewater-treatment processes in the chemical sector. *Environ. Sci. Technol.* **41**, 5515–5522 (2007).
  67. Köhler, A. Environmental Assessment of Industrial Wastewater Treatment Processes and Waterborne Organic Contaminant Emissions. (ETH, 2006). doi:10.3929/ETHZ-A-005206273
  68. Wernet, G., Conradt, S., Isenring, H. P., Jiménez-González, C. & Hungerbühler, K. Life cycle assessment of fine chemical production: A case study of pharmaceutical synthesis. *Int. J. Life Cycle Assess.* **15**, 294–303 (2010).
  69. Sharma, R. K., Sarkar, P. & Singh, H. Assessing the sustainability of a manufacturing process using life cycle assessment technique—a case of an Indian pharmaceutical company. *Clean Technol. Environ. Policy* **22**, 1269–1284 (2020).
  70. Sphera. LCA for Experts Software (fka GaBi). Available at: <https://sphera.com/life-cycle-assessment-lca-software/>. (Accessed: 24th August 2023)
  71. Wernet, G. *et al.* The ecoinvent database version 3 (part I): overview and methodology. *Int. J. Life Cycle Assess.* **21**, 1218–1230 (2016).
  72. Pulp mills | UPM Pulp. (2022). Available at: <https://www.upmpulp.com/about-upm-pulp/pulp-mills/>. (Accessed: 3rd May 2022)
  73. Boutekdjiret, C., Vian, M. A. & Chemat, F. Terpenes as Green Solvents for Natural Products Extraction. in 205–219 (2014). doi:10.1007/978-3-662-43628-8\_9
  74. Cordova, A. Terpene/co-solvent adhesive or paint coating composition for toy articles. (2001).
  75. Soares, A. & Pestana, M. Polyterpene Resins: Part I – A Brief Historical Review. *Silva Lusit.* **28**, 181–195 (2020).
  76. Yildirim, E., Emsen, B. & Kordali, S. Insecticidal effects of monoterpenes on *Sitophilus zeamais* Motschulsky (Coleoptera: Curculionidae). *J. Appl. Bot. Food Qual.* **86**, 198–204 (2013).
  77. Wholesale Terpenes For Sale | Buy Bulk Terpenes | Lab Effects. Available at: <https://labeffects.com/>. (Accessed: 18th January 2022)
  78. Tetali, S. D. Terpenes and isoprenoids: a wealth of compounds for global use. *Planta* **249**, 1–8 (2019).
  79. Zielińska-Błajet, M. & Feder-Kubis, J. Monoterpenes and their derivatives—recent development in biological and medical applications. *International Journal of Molecular*

*Sciences* **21**, 1–38 (2020).

80. Salehi, B. *et al.* Therapeutic potential of  $\alpha$ -and  $\beta$ -pinene: A miracle gift of nature. *Biomolecules* **9**, (2019).